MAUSAM, **76**, 1 (January 2025), 185-214

MAUSAM

DOI : https://doi.org/10.54302/mausam.v76i1.6941
Homepage: https://mausamjournal.imd.gov.in/index.php/MAUSAM

UDC No. 502:551.5

Advances in environmental meteorology and air quality early warning

K. J. RAMESH, CHINMAY JENA*, ANIKENDER KUMAR*, VIVEK KUMAR* and V. K. SONI*

Former Director General, India Meteorological Department, MoES New Delhi

**India Meteorological Department, Ministry of Earth Sciences, New Delhi, India*

e mail : soni_vk@yahoo.com

सार – 1875 में स्थापित भारत मौसम विज्ञान विभाग के पास जलवायु और पर्यावरण मापदंडों की निगरानी की एक लंबी विरासत है। आईएमडी भारत में सौर विकिरण, ओजोन, वर्षा रसायन विज्ञान और एरोसोल ऑप्टिकल और भौतिक गुणों और वायुमंडलीय रसायन विज्ञान का व्यवस्थित दीर्घकालिक अवलोकन शुरू करने वाला पहला संस्थान था। सौर विकिरण मापन पहली बार नवंबर 1879 में कोलकाता में शुरू हुआ था। हालाँकि, अंतर्राष्ट्रीय भूभौतिकीय वर्ष 1957-58 के बाद दुनिया भर में विभिन्न भूभौतिकीय घटनाओं के समन्वित और व्यवस्थित अवलोकन की एक श्रृंखला शुरू हुई। स्वतंत्रता के बाद आईएमडी मौसम संबंधी उपकरणों के निर्माण के पूर्ण स्वदेशीकरण की मांग को पूरा करने के लिए आगे आया। आईएमडी ने अंतरराष्ट्रीय स्तर पर स्थापित निर्माताओं के बराबर निर्दिष्ट सटीकता के साथ मौसम विज्ञान, विकिरण और ओजोन माप उपकरणों का निर्माण शुरू किया। भारत मौसम विज्ञान विभाग के पास ओजोन के सभी तीन घटकों यानी कुल स्तंभ ओजोन, ऊर्ध्वाधर वितरण और सतह ओजोन माप के माप का लंबा इतिहास है। भारत में कुल स्तंभकार ओजोन माप पहली बार सितंबर 1928 से अगस्त 1929 के दौरान आईएमडी की कोडाइकनाल वेधशाला में किया गया था। मौसम और जलवायु पूर्वानुमान की तुलना में आईएमडी में वायु गुणवत्ता पूर्वानुमान अपेक्षाकृत बहुत नई पहल है। वायु गुणवत्ता प्रारंभिक चेतावनी प्रणाली (AQEWS) अत्यधिक प्रदूषण अलर्ट को कम करने, निर्णय लेने और सार्वजनिक स्वास्थ्य सुरक्षा में सहायता करने के लिए प्रदूषण नियंत्रण अधिकारियों को वास्तविक समय डेटा और प्रारंभिक चेतावनी प्रदान करती है। यह पेपर पर्यावरण मौसम विज्ञान में उभरते रुझानों और वायुमंडलीय पर्यावरण की निगरानी और भविष्यवाणी में आईएमडी की महत्वपूर्ण भूमिका की समीक्षा करता है।

ABSTRACT. India Meteorological Department (IMD) established in 1875 has a long legacy of monitoring climate and environmental parameters. IMD was the first institution in India to start systematic long-term observation of Solar Radiation, Ozone, Precipitation Chemistry and optical, physical, and physical proprieties of aerosol. The solar radiation measurement started for the first time at Kolkata as early as November,1879. However, a series of coordinated and systematic observations of various geophysical phenomena started all over the globe after International Geophysical Year (IGY) 1957-58. Post-independent IMD rose up to meet the demand for enhancing the density of observing systems through a self-reliant approach of total indigenization of the manufacture of meteorological instruments. IMD started manufacturing meteorological, radiation and ozone measurement instruments to the specified accuracy at par with the internationally established manufacturers. IMD has long history of measurement of all the three components of Ozone *i.e.* Total Columnar Ozone, Vertical Distribution and Surface Ozone measurement. Total Columnar Ozone measurements in India were first made during September 1928 to August 1929 at Kodaikanal observatory of IMD. The air quality forecast is relatively recent initiative in IMD compared to digital weather and climate forecasts generation. The Air Quality Early Warning System (AQEWS) provide real-time forecast products for early warning of changing profile of Air Quality Index (AQI) across the National Capital Region (NCR) of Delhi to designated air quality management/regulatory authorities in order to moderate anticipated high AQI levels through enforcing various sector targeted emission reduction actions specified under graded response action plans (GRAP). This paper reviews emerging trends in environment meteorology and IMD's pivotal role in monitoring and prediction of atmospheric environment.

Key words – Precipitation chemistry, Ozone, Solar radiation, Aerosol, AQEWS.

1. Introduction

In the 1950s, World Meteorological Organization (WMO) formally started a programme on atmospheric chemistry and the meteorological aspects of air pollution that transformed early sporadic measurements into regular observations. This programme ensured adequate collection of such data and analysis of its anthropogenic impact on a global scale. The programme harmonized by expressing the atmospheric composition in the same units and on the same

scale, so that measurements carried out by different countries could be comparable. WMO assumed responsibility for standard procedures for uniform ozone observations and established the Global Ozone Observing System (GO3OS) during the International Geophysical Year, 1957. The GO3OS was responsible for ozonesonde inter-comparisons, preparation of the ozone bulletins and ozone assessments and support of the Ozone Data Centre in Toronto, Canada (now World Ozone and Ultraviolet Radiation Data Centre, WOUDC). The Organization also coordinated the Dobson and later Brewer, spectro-photometer network to measure total columnar ozone. In the late 1960s, the Background Air Pollution Monitoring Network (BAPMoN) was established by WMO, focusing on precipitation chemistry, aerosol and carbon dioxide measurements. The Network included regional and background stations and a WMO World Data Centre was established in the United States of America. IMD joined the BAPMoN efforts during 1970s with the establishment of ten stations of precipitation chemistry in India.

IMD, established in 1875, has always been playing a pioneering role in meteorological and atmospheric observations and associated research studies in India. Initially focused on weather forecasting and seismology, the department gradually expanded its scope to include climate research, disaster management, and environmental monitoring & air quality forecasting. Recognizing the importance of atmospheric composition, IMD became an active participant in global atmospheric observation programs like BAPMoN. Over the years, IMD has established itself as a global partner for implementing atmospheric environment monitoring systems expansion and thereby contributing towards sustained measurement of solar radiation, atmospheric aerosols, ozone and precipitation chemistry over India

During the 1970s, three important atmospheric issues were addressed by WMO through GO3OS, BAPMoN and meteorological network: (*i*) the threat of chlorofluorocarbons (CFCs) to the ozone layer, (*ii*) the acidification of lakes and forests, caused principally by the conversion of sulphur dioxide into sulphuric acid by precipitation processes in the atmosphere, and (*iii*) global warming caused by the build-up of greenhouse gases in the atmosphere. Each of these issues have become now the subject of international treaties or conventions such as Viena Convention, UNFCCC *etc*. The initial development of these agreements and the subsequent assessments of the mitigation measures relied on the information derived from the WMO atmospheric composition observations and analysis programme. In 1989, the two observing networks, BAPMoN and GO3OS, were consolidated into the current WMO Global Atmosphere Watch (GAW) Programme. As the networks evolved and grew, so did the community involved in atmospheric composition observations and analysis. Recognizing the critical role of aerosols in climate systems, IMD initiated systematic long-term measurements of aerosol optical properties using broadband optical filters. The introduction of sun-photometers at multiple locations in India in campaign mode marked advancement in aerosol monitoring. Key studies during this period identified high aerosol concentrations over the Indo-Gangetic Plain and their impact on the regional climate.

IMD has been continuously expanding and integrating its programs with the WMO's GAW, focusing on harmonized atmospheric composition measurements. It expanded its observational network to include advanced instruments such as nephelometers, aethalometers, and skyradiometers for detailed characterization of aerosols and black carbon. IMD's studies on black carbon have revealed its significant role in regional climate warming and monsoon variability. Long-term trends analyzed by IMD have shown a declining trend in black carbon concentrations, indicating the success of certain mitigation measures. In 2012, IMD established a nationwide 12-nation network of Sky Radiometers that was subsequently expanded to 20-stations in 2020 to enhance the understanding of aerosols' impact on weather, climate, air quality and public health. The program established a continuously operating observational network across India and thereby enabling advanced research on aerosol-radiation interactions.

Concurrently, IMD has been leveraging satellite data for real-time atmospheric composition monitoring. Its collaborations with ISRO and other agencies have enhanced India's capabilities in tracking aerosols, greenhouse gases, and ozone levels. IMD has been instrumental in monitoring urban air quality in partnership with its sister organization, Indian Institute of Tropical Meteorology (IITM), particularly in megacities like Delhi, Pune, Ahmedabad and Pune where it provides air quality forecasts and real-time data to policymakers and the public. Such efforts have contributed to the formulation of various public health safety initiatives by disseminating information on air quality for minimizing adverse implications over public health.

IMD's collaboration with WMO's programs like GAW further strengthened its capacity to study and address atmospheric composition. Leveraging its historical expertise and infrastructure, IMD has undertaken numerous initiatives, including the establishment of advanced monitoring networks, to study aerosols, greenhouse gases, and other critical atmospheric parameters. This historical progression underscores the vital role of IMD in contributing to the global understanding of atmospheric processes while addressing region-specific challenges.

2. Advances in atmospheric monitoring

2.1. *Ozone monitoring*

The first network for daily ozone measurements was initiated by G. M. B. Dobson from Clarendon Lab of the University of Oxford. Utilizing a UV quartz spectrograph based on Fabry and Buisson's (1913) method, Dobson built six ozone spectrographs with support from the Royal Society London (Dobson and Harrison, 1926; Féry, 1911). These spectrographs were dispatched to various meteorological agencies worldwide between 1925 and 1930 to study atmospheric ozone variations and explore its potential for weather forecasting. Observations were collected from locations such as in 1926-27 Abisko (SW), Lerwick (UK), Valentia (IR), Oxford (UK), Lindenberg (GE), Arosa (CH) and Montezuma (Chili); in 1928-30 from Oxford (UK), Arosa (CH), Table Mountain (USA), Helwan (EG), Kodaikanal (IN) and Christchurch (NZ). These foundational measurements analyzed ozone variations by latitude, seasons, and weather, forming the basis of global ozone studies until the International Geophysical Year (IGY) when regular systematic ozone observations were started on a global basis.

IMD has a long history of measuring all three components of ozone: Total Columnar Ozone (TCO), Vertical Distribution, and Surface Ozone. The first TCO measurements in India were conducted between September 1928 and August 1929 by Dr. Royds and Dr. Narayan at Kodaikanal, as part of Dobson's global ozone measurement program using his spectrograph and the method of photographic photometry (Dobson *et al*., 1930). Subsequently, Chiplonkar (1939) utilized the same photographic instrument for daily ozone measurements at the Colaba Observatory, Bombay (now Mumbai), from October 1936 to September 1938, confirming seasonal variation patterns consistent with the Kodaikanal results. These early studies established the existence of low total columnar ozone values over the tropical region. The introduction of Dobson's photo-electric spectrophotometer marked a significant advancement in ozone measurement, offering greater sensitivity, accuracy and ease of use compared to photographic methods. This instrument also enabled measurements of vertical distribution of ozone using the Umkehr Effect. Götz (1931) found that the ratio of zenith sky radiances of two wavelengths in the Sun's ultraviolet radiation, one strongly and the other weakly absorbed by ozone, increases with increasing solar zenith angles but suddenly decreases at zenith angles close to 90o. This is known as Umkehr effect and such measurements contain information about the vertical distribution of ozone in the stratosphere (Götz *et al*., 1934). IMD acquired its first Dobson spectrophotometer in 1940, initiating regular ozone measurements. Observations with the new instrument began at Poona (Pune) in February 1940 by Ramanathan, Ananthakrishnan and Venkateshwaran, who obtained Umkehr curves over six clear days during February and March. However, these measurements were interrupted until 1945 due to 2nd world wartime constraints. Systematic observations resumed in Delhi between November 1945 and March 1947 (Karandikar, 1948), yielding 35 Umkehr curves despite challenges posed by the summer haze in northwestern India. The study provided results on vertical profile of ozone using Umkehr Effect despite of the fact that in low latitudes the height of the sun changes rapidly when it is near the horizon making it difficult to take accurate and many observations at sunset or sunrise; still, the observations were good enough to indicate the existence of the 'Umkehr Effect'. In April 1947, the instrument was moved to Shimla to compare its performance under reduced haze and dust conditions. At Shimla, 15 Umkehr curves were recorded during April-May and an additional 9 curves were obtained in November 1947. The instrument was then relocated back to Poona, where further measurements were conducted during February-March 1948 under clear skies. Professor Ramanathan made significant contributions in the studies of atmospheric ozone. Ramanathan, (1963) discovered the bi-annual variation of atmospheric ozone over the tropics using the observations of total ozone over Mt. Abu/ Ahmedabad, Kodaikanal, Tateno, Rome, Aspendale and Brisbane. He showed that there is a bi-annual variation of atmospheric ozone over equatorial, subtropical and lower middle latitude stations, a year of high ozone being followed by one of low ozone. A high ozone year in the sub-tropics and lower middle latitudes corresponds to a year of low ozone near the equator.

In subsequent years, IMD established a network for boosting ozone research, focusing on all the components *i.e*. surface ozone, TCO and vertical distribution of ozone (Fig. 1). IMD expanded ozone network by deploying Dobson spectrophotometers to cover different latitudes across India. These instruments facilitated long-term monitoring of total ozone levels and contributed to the study of seasonal and spatial ozone variations over the Indian subcontinent. The data from this network are also archived at World Ozone and Ultraviolet Radiation Data Centre (WOUDC). IMD also acquired more advanced instruments, such as Brewer spectrophotometers and ozone sondes, for improved accuracy in measuring ozone concentration and its vertical distribution in India (Ramanathan, 1961; Ramanathan *et al*., 1965; Rangarajan, 1963; Peshin *et al*., 2000, 2003; Sharma *et al*., 2011; Sinha *et al*., 2016) and also in Antarctica (Kumar *et al*., 2023a; Lal and Ram, 2013; Peshin *et al*., 1997; Soni *et al*., 2017; Tiwari, 1999). Pathakoti *et al*., (2021) studied the TCO trends indicating increasing trend of TCO values over Delhi. Using long - term data, Pathakoti *et al.* (2018)

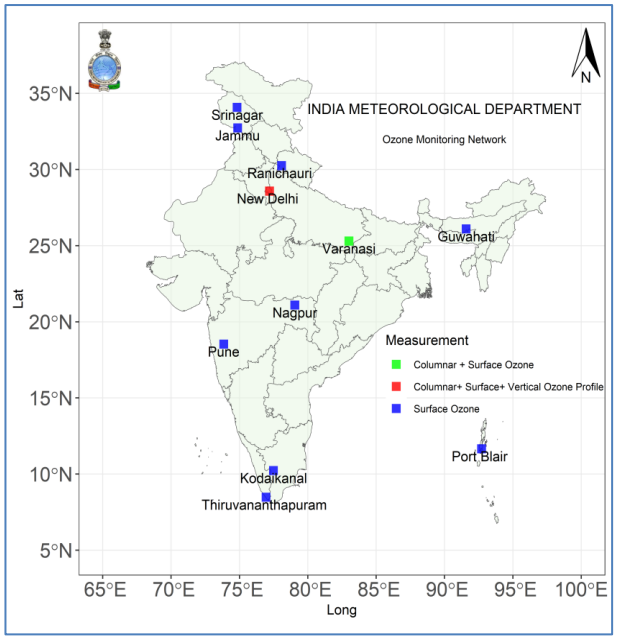

Fig. 1. IMD network for Ozone monitoring

observed a quantitative rate of TCO increase per decade respectively over New Delhi (1.41%), Pune (1.96%) and Kodaikanal (1.53%) and decreasing trend over Varanasi (-1.61%).

Total column ozone values at all the monitoring stations are greatly influenced by the solar radiation, having higher values during summer months and lower values in winter months in Northern Hemisphere. This implies, in general, that the dominant factor controlling the concentration of total Ozone is photochemistry. The daily averaged total column ozone for Delhi, Kodaikanal, Varanasi, Pune, Srinagar and Maitri ranges from 196 - 368, 210 - 286, 227 - 304, 226 - 290, 209 - 300 and 113 - 348 DU respectively. The monthly mean values of TCO at different stations are depicted in Fig. 2.

IMD tested the first successful ozone-sounding from Pune in September 1964 using IMD make Ozonesonde. The first Indian balloon-borne electrochemical ozonesonde was developed under the supervision of Ms. Anna Mani in 1964 and the first surface ozone recorder in 1970 at the Instruments Division of the Meteorological Office at Poona (now Pune). The IMD make ozonesonde is a modified version of the Brewer electrochemical sonde. The ozone sensor transmits values of air temperature, air pressure, relative humidity, detector current, detector temperature, and pump speed to a ground receiving station. The air containing the ozone sample is pumped through Potassium Iodide solution which is oxidized by ozone producing an electrical current. The electrical current is proportional to the flow of ozone. The instrument became operational at the India Meteorological Department in 1971. During the

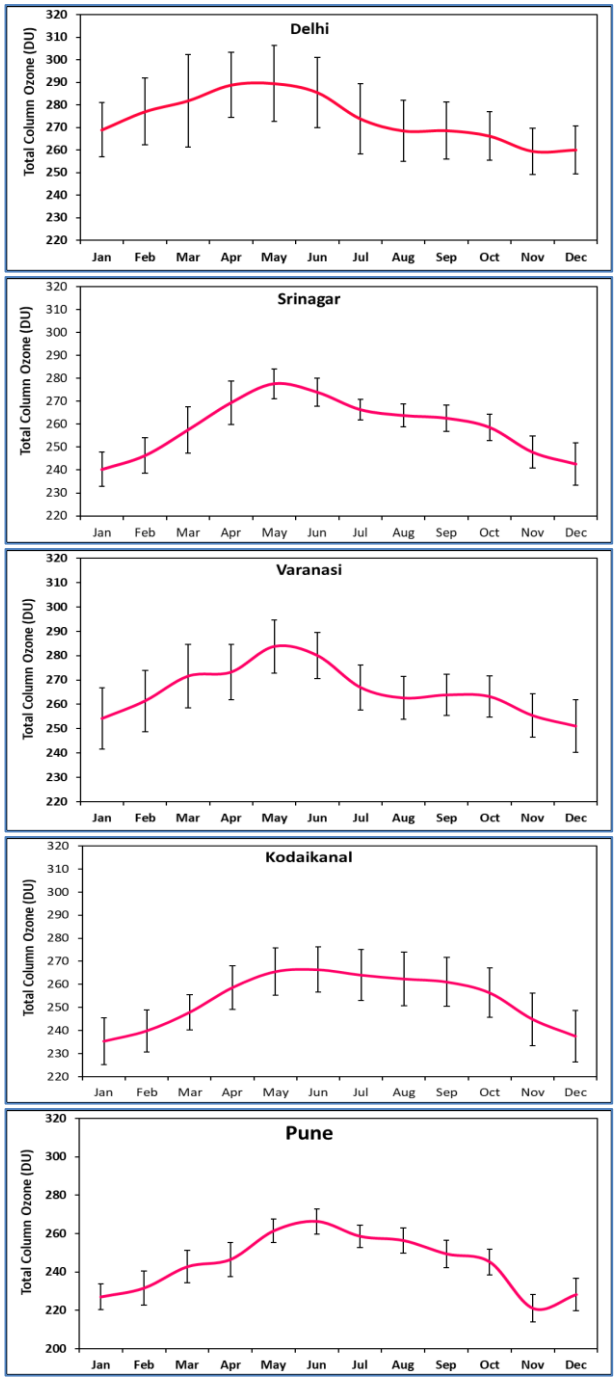

Fig. 2: Monthly variation of Total Column Ozone at Delhi, Srinagar, Varanasi, Kodaikanal and Pune using Dobson Spectrophotometer

next five years the sonde was improved to such an extent that systematic soundings were started from Thiruvananthapuram, Pune and New Delhi. In 1970 the Indian ozone-sonde was inter-compared in the International Ozone-sonde inter-comparisons held in Germany. IMD started ozone monitoring over Antarctica since second expedition (1982-83) during which Ozonesonde ascents

were taken to obtain the vertical profile of ozone at the Indian station using IMD make electro-chemical ozonesonde. IMD further strengthened the ozone observations at Dakshin Gangotri to join the international efforts for Antarctica Ozone-Hole Investigation. In 1974, Molina and Rowland published their theory about catalytic destruction of ozone involving CFCs. In 1985, Joe Farman, Brian Gardiner and Jonathan Shanklin reported large decreases in stratospheric ozone levels over the Antarctic stations of Halley and Faraday which led to the discovery of Ozone Hole. Global efforts were mobilized for the systematic measurement of atmospheric ozone. The ozone soundings had become a routine part of the Indian scientific expeditions to Antarctica from second expedition (1982-83) onwards almost three years before discovery of ozone hole. The Indian ozone sounding clearly showed the 'ozone hole' over Antarctica and corroborated Farman's discovery. The soundings have yielded an accurate assessment of the vertical distribution of ozone in the tropics and its temporal and spatial variations. The soundings over Antarctica provided clear evidence of the dramatic ozone depletion. Subsequently, Montreal Protocol, came in to existence in 1987, to protect the stratospheric ozone layer by phasing out the production and consumption of ozone depleting substances. Regular ozone profile measurement continued at Dakshin Gangotri till it was abandoned in 1989. The surface and profile ozone observations started at second station Maitri. Brewer Spectrophotometer was operated at Maitri, from 1999 to 2011 for the measurement of TCO. The ozone measurement programme started at third Indian Antarctic stations Bharati from 2015. The Indian ozone soundings assume special significance because India is the only country conducting systematic ozone measurements from the tropical and Antarctic region. All other countries that make ozone soundings do it from the middle and high latitudes. Surface ozone is also measured at Indian stations in Antarctica. As anthropogenic pollution is almost negligible at Maitri, the in-situ photochemical production of ozone may not be very significant. Depletion in the stratospheric ozone during ozone hole period gives way to highly energetic UV radiation to reach to the surface layer and initiate photolysis of oxygen and NOx molecules in the surface boundary layer leading to production of surface ozone. The NOx is produced from surface snow pack. Moreover, the surface ozone concentrations can also be increased by the downward transport of stratospheric ozone rich air during deep convection and stratosphere-to-troposphere exchange event. Episodes of high surface ozone in the Antarctica region associated with stratospheric intrusion have been reported at Maitri.

From 1999 to 2011, a Brewer Spectrophotometer (Mark IV, No. 153) operated at Maitri measured total column ozone (TCO), as well as total column densities of NO_2 and SO_2 and UV-B flux. Peshin (2011) reported increased SO_2 during ozone-hole events, attributed to UV-B penetration into the troposphere, which dissociates in the upper atmosphere, enhancing SO_2 production. NO_2 column densities also increased during spring, linked to longer daylight hours as austral summer approached. Surface ozone at Maitri is measured using the Electrochemical Conductivity Cell method. Diurnal variation is minimal (~5 ppbv) during October-February due to consistent solar radiation, with smaller variations during polar nights compared to polar days. Ali *et al*. (2017) observed daily surface ozone levels of 13-20 ppbv at Larsemann Hills (average ~16 ppbv) and 16-21 ppbv at Maitri (average ~18 ppbv). Surface ozone, a secondary pollutant, forms through oxidation of precursor gases (*e.g*., CO or hydrocarbons) in the presence of NO_x. At Maitri, anthropogenic pollution is negligible, limiting photochemical ozone production. However, stratospheric ozone depletion during ozone-hole periods allows UV radiation to reach the surface, triggering photolysis of oxygen and NO_x, with NO_x primarily produced from snowpack nitrate photolysis. Stratosphere-to-troposphere exchange and deep convection also transport ozone-rich air downward, occasionally causing high surface ozone episodes in Antarctica (Ganguly, 2013).

2.2. *Precipitation chemistry over Indian region*

Atmospheric deposition has been a major research focus in national and international programs. The phenomenon of acid rain dates back at least three centuries. As early as 1692, Robert Boyle identified sulfur compounds and acids in air and rain, which he described as "nitrous or salino-sulfurous spirits." In 1853, Robert Angus Smith coined the term "acid rain" after studying rain chemistry in Manchester, UK published in *Air and Rain: The Beginnings of Chemical Climatology* in 1872. By the late 19th century, sulfur dioxide emissions from industrial sources in the United Kingdom were recognized as contributors to the long-range transport of pollutants, which caused the bleaching of dyed cloth in France (U.S. NAPAP, 1991).

In India, concerns about airborne pollution and its impact on ecosystems gained prominence in the mid - 20^{th} century. Precipitation chemistry studies began in the 1950s, prior to the WMO BAPMoN program. Mukherjee (1978, 1964, 1957, 1956) found that monsoon rainwater pH in Calcutta, Bombay and the Bay of Bengal ranged between 6.0 and 7.0 which are the earliest studies in India. Mukherjee (1956) derived an equation correlating salt concentration in rainwater with rainfall amount, aligning with global research findings. Handa, 1969 reported pH values ranging from 4.8 to 7.15 for monsoon rainwater in Calcutta, including the first recorded instance of acid rain in India, with a pH of 4.4 observed in September 1967 for the samples collected during 1967-68 at Calcutta. The first

study of monsoon rainwater pH over the Bay of Bengal was conducted by (Mukherjee, 1978) aboard the USSR research ship *Akademic Shirshov* during Monex-1977.Other early studies byMukherjee, (1964), Handa (1968, 1969, 1971), Verma *et al*. (1970), Sadasivan, (1979, 1980), Das *et al*., (1981) and Handa *et al*. (1982) reported the chemical composition of rainwater across different regions, revealing localized trends due to meteorological and anthropogenic factors.

With the commencement of the GAW (formerly BAPMoN) program, IMD achieved broader spatial and temporal coverage of precipitation chemistry network in 1970s as depicted in Fig. 3. The GAW network consists of 10 stations (*e.g*., Allahabad/Prayagraj (ALB), Jodhpur (JDP), Kodaikanal (KDK), Minicoy (MNC), Mohanbari (MHB), Nagpur (NGP), Port Blair (PBL), Pune (PNE), Srinagar (SRN), Visakhapatnam (VSK)), maintained according to WMO standards. One more station Ranichauri, Uttarakhand was added to this network in 2009. Rainwater chemistry has been extensively studied using observed data from IMD's precipitation chemistry network (Maske and Nand, 1982; Mukherjee *et al*., 1986; Nand, 1984, 1986; Mukhopadhyay *et al*., 1992, 1993; Sarkar *et al*., 2006; Soni *et al*., 2006; Vizaya Bhaskar and Rao, 2017; Bhaskar *et al*., 2022) over the past decades, Maske and Nand (1982) identified Cl^-, Na^+, SO_4^{2-}, NO_3^-, Ca^{2+} and K^+ as major rainwater constituents, with maritime air and anthropogenic sources as key contributors. Soil-derived aerosols influenced pH, especially in Jodhpur. Mukherjee *et al*., (1986) found that maritime air was a dominant source of Cl^- and Na^+ at Minicoy and Port Blair, with basic pH values indicating limited influence of HNO_3 and H_2SO_4. Most GAW stations, except Jodhpur, show a decreasing pH trend, with values dropping from around 7.0 in the 1980s to 5.0-6.0 by 2000. The pH values vary geographically, Jodhpur (6.6-7.8), Allahabad (5.2-7.6) and Mohanbari (4.5-6.8). Marine aerosols govern rainwater acidity at coastal stations, while soil-derived aerosols in arid regions like Jodhpur maintain higher pH levels. Organic acids from vegetation significantly influence rainwater pH at stations like Kodaikanal and Mohanbari. Industrialization and urbanization have led to increased sulfate and nitrate concentrations in rainwater, with significant impacts observed in cities like Pune and Visakhapatnam. Wind-blown soil particles, ammonium, and maritime sources buffer pH levels in many non-polluted areas. Sensitive regions like northeastern India and the west coast of the southern peninsula exhibit lower pH values (4.0-5.0) due to acidic soils and occasional pollution stagnation. Decadal analysis indicates rising sulfate and nitrate concentrations, though India remains better off compared to many countries in terms of acid rain threats. Chemicals present in the atmosphere influence the

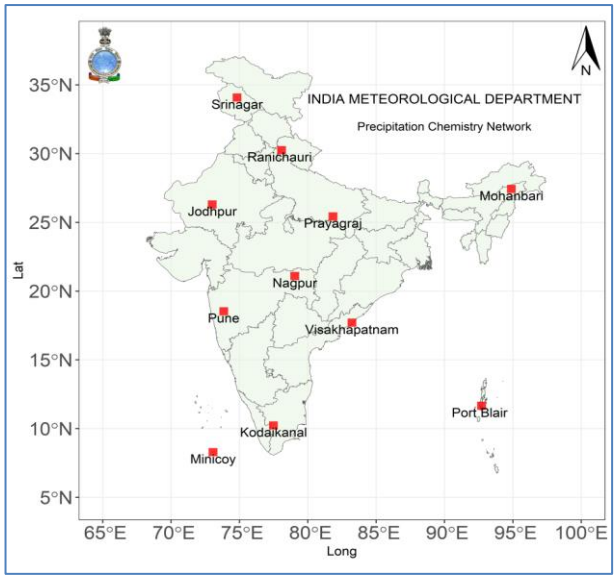

Fig. 3. IMD network for Precipitation Chemistry

chemical characteristics of rainwater whereas the material deposited by the rain affects soil, surface water and vegetation. In view of this, IMD has planned to strengthen the existing precipitation chemistry network by inducting modern technology in sample collection and chemical analysis of rainwater. IMD also has planned to augment the network by establishing more stations at background locations in all climatic zones of India. The data generated will significantly contribute to the limited knowledge available on chemical composition of precipitation over Indian region.

The pH of rainwater is influenced by ion concentration of nitrates, sulphate and carbonate as the increase in atmospheric concentration of gases (SO_2, NOx) causes to decrease the pH of rainwater due to increase in quantity of nitric acid, sulphuric acid and carbonic acid in the rainwater. The acidic pH reveals the presence of strong acids while neutral or alkaline pH indicates neutralization of acids by carbonates, mineral dust or by ammonium. Fig. 4(a) highlights the decadal mean concentrations of nitrate (NO_3^-) and sulphate (SO_4^{2-}) at monitoring stations. The data are segmented into three decades: 1991-2000, 2001-2010 and 2011-2020 to discern the trend. For nitrate (top panel), a significant spatial and temporal variability is evident. The mean concentration of nitratein rainwater increased at stations JDP, KDK, MHB, PNE and SRN in later decade 2011-2020 during wet season. The increase in nitrate levels in rainwater can be attributed to emissions driven by anthropogenic activities such as fossil fuel combustion and vehicular emissions. The sulphate concentration in rainwater showed marginal rise or decline at most of the stations, indicating potential sources like industrial emissions or increased urbanization. Fig. 4(b)

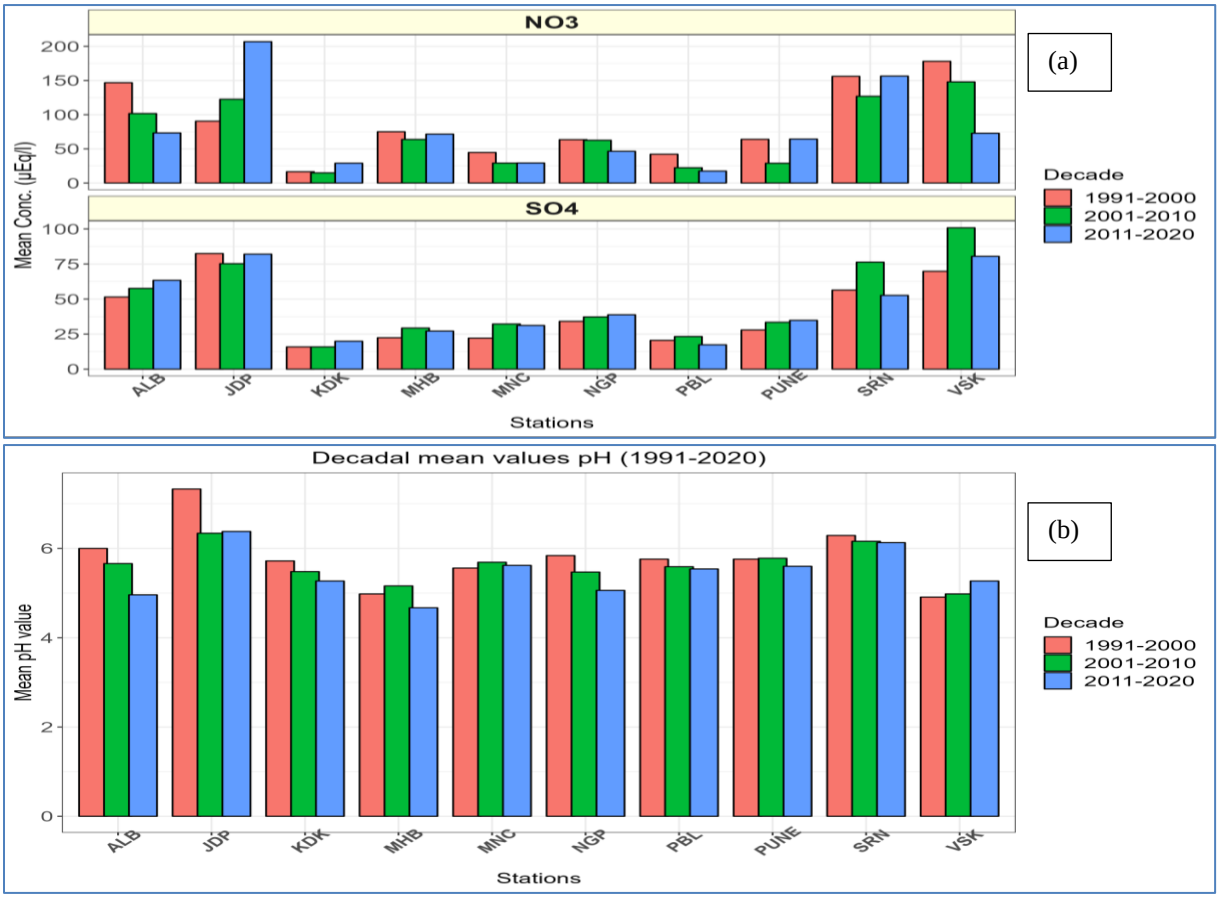

Figs .4 (a&b). Decadal Trends in **(a)** Nitrate, Sulphate and **(b)** Rainwater pH across Precipitation Chemistry Network of IMD (1991-2020)

illustrates the decadal mean pH values of precipitation at the same stations for the corresponding decades. The pH values are largely neutral or slightly acidic at all the ten stations. The decadal mean pH values show marginal decline at most of the stations except Jodhpur, Srinagar and Visakhapatnam in later decade 2011-2020.

The decadal trends in precipitation pH across the IMD network (Table 1) indicate a gradual reduction in acidity of rainwater over time, with notable differences between seasons and locations. The Table 1-3 presents pH, Sulphate and Nitrate in rainwater during wet (June -September) and dry seasons (October, November, December, January, February and March). The stations ALB, JDP, KDK, MHB, NGP and SRN show increasing trend in pH during the decade 2011-2020 for wet season. This indicates a gradual decline in acidic character of rainwater in later decade. The sulphate concentrations declined or marginally increased at all the stations, especially in recent years, whereas nitrate levels were somewhat stable or increased slightly. The stations Minicoy, Port Blair and Visakhapatnam showed non-significant declining trend during wet season. These findings suggest that emission controls and local meteorological conditions play a key role in modulating acidity of rainwater.

The trends in sulfate concentrations highlight distinct patterns across the IMD precipitation chemistry network, influenced by anthropogenic and natural sources. During the wet season, substantial reductions in sulfate levels are evident in urban or semi-urban areas (Table 2), such as Jodhpur (-5.07 in 1991-2000), reflecting the impact of sulfur dioxide emission controls and cleaner fuel use. However, stations like Mohanbari show marginal positive trends across decades (*e.g.*, 0.15 for 1991-2000), suggesting consistent local or regional emissions, possibly linked to industrial activity. In the dry season, significant reductions in sulfate levels are observed at Srinagar (-11.09 in 1991-2000 to -0.64 in 2011-2020), underscoring the success of pollution mitigation strategies. The inconsistencies persist at remote stations like Minicoy, where trends fluctuate due to variable contributions from marine and local anthropogenic sources. These results reveal the heterogeneous response of sulfate concentrations to emission control measures, with urban areas benefiting more, while remote locations reflect a mix of regulated and unregulated sources.

TABLE 1

Decadal trend of pH at stations in IMD precipitation chemistry network

	WET SEASON			DRY SEASON		
Stations/Decade	1991-2000	2001-2010	2011-2020	1991-2000	2001-2010	2011-2020
Prayagraj	**-0.14**	-0.07	0.03	**-0.21**	-0.09	-0.06
Jodhpur	-0.09	-0.06	0.02	-0.05	0.02	**0.22**
Kodaikanal	**-0.09**	0.00	0.06	-0.07	0.01	0.05
Mohanbari	0.04	-0.01	0.08	-0.04	-0.06	0.05
Minicoy	**-0.20**	0.04	-0.01	**-0.13**	0.07	**-0.06**
Nagpur	**-0.10**	-0.04	0.03	-0.10	-0.03	0.16
Port Blair	-0.09	-0.02	-0.07	-0.04	0.02	-0.02
Pune	-0.07	-0.04	-0.02	-0.05	-0.04	0.03
Srinagar	**-0.12**	0.05	0.09	**-0.19**	**0.12**	0.05
Visakhapatnam	0.00	0.04	-0.05	0.02	-0.04	**0.08**

Significant values at 90 % confidence interval are in bold fonts.

TABLE 2

Decadal trend of Sulphate concentration (µEq/l) in rainwater over stations in IMD precipitation chemistry network

	WET SEASON			DRY SEASON		
Stations/Decade	1991-2000	2001-2010	2011-2020	1991-2000	2001-2010	2011-2020
Prayagraj	0.09	**-8.84**	-0.75	6.07	-5.36	-2.68
Jodhpur	-5.07	-5.52	6.92	12.69	-7.00	-8.51
Kodaikanal	-0.06	-0.89	0.07	0.53	**-0.91**	0.42
Mohanbari	0.15	0.13	0.13	0.72	1.68	1.25
Minicoy	0.73	-1.29	3.59	1.82	0.77	0.89
Nagpur	**3.82**	-1.72	0.21	**6.44**	-3.32	2.14
Port Blair	**2.25**	-0.57	-0.06	0.58	-0.37	0.18
Pune	1.18	**-2.21**	1.04	-0.26	3.89	8.87
Srinagar	**9.24**	7.60	**-5.62**	**11.09**	0.04	-0.64
Visakhapatnam	**5.74**	9.47	1.40	6.28	-1.58	-5.31

Significant values at 90 % confidence interval are in bold fonts.

TABLE 3

Decadal trend of Nitrate concentration (µEq/l) in rainwater over stations in IMD precipitation chemistry network

	WET SEASON			DRY SEASON		
Stations/Decade	1991-2000	2001-2010	2011-2020	1991-2000	2001-2010	2011-2020
Prayagraj	**-23.13**	**-9.30**	9.64	-44.58	-3.25	-0.11
Jodhpur	13.50	-9.26	42.59	-19.07	-8.17	-17.41
Kodaikanal	0.33	-1.01	2.87	0.59	**-1.73**	1.92
Mohanbari	**-5.15**	**6.61**	1.94	-20.72	-2.27	12.46
Minicoy	-7.49	0.25	10.79	-1.40	1.55	3.32
Nagpur	3.03	-2.33	6.15	-4.04	-2.77	**-25.62**
Port Blair	**8.42**	-1.12	4.05	**7.87**	-1.16	2.63
Pune	-0.53	-0.36	4.39	-8.46	6.39	16.65
Srinagar	-18.98	4.97	16.21	-21.01	0.93	17.89
Visakhapatnam	-14.64	1.86	14.74	-1.02	2.95	-1.73

Significant values at 90 % confidence interval are in bold fonts.

The nitrate trends over the decades (Table 3) exhibit substantial variability, reflecting the complex interplay of nitrogen oxides (NO_x) emissions and environmental processes. In the wet season, several stations, exhibit a marked reduction in nitrate levels during earlier decades. However, certain locations, such as Jodhpur, show an increase in nitrate trends in the later decades, suggesting a rise in industrial or agricultural activities contributing to nitrogen emissions. During the dry season, an increasing trend is noted at stations Srinagar and Mohanbari, with consistent positive changes in the later decades. This contrasts with significant reductions observed at Nagpur, which point to the success of emission control efforts in certain regions. The variability in trends reflects a combination of anthropogenic influences, such as vehicular emissions, industrial activities and agricultural sources, coupled with local atmospheric conditions, which modulate nitrate deposition across seasons and locations.

3. Atmospheric aerosols and climate impact

Aerosols consist of various forms of chemical compounds which have different optical properties. Atmospheric aerosols affect the Earth's radiative balance directly by scattering Charlson *et al*. (1991, 1992) and absorption of solar radiation (Satheesh and Ramanathan, 2000) and indirectly by acting as cloud condensation nuclei, thereby influencing the albedo (Twomey or cloud albedo effect), lifetime (Albrecht effect or cloud lifetime effect) and precipitation of clouds (Ramanathan *et al*., 2001). Study of the optical and physical properties of aerosol particles is important for assessment of their effect on climate and for development of more accurate remote sensing procedures of aerosols from satellite sensors. The quantification of aerosol radiative forcing is highly complex because aerosol mass and particle number concentrations are highly variable in space and time. This variability is largely due to the much shorter atmospheric lifetime of aerosols (few hours to a week) and the numerous ways they interact with other elements of the climate system (Kaufman *et al*., 2002). The radiative effects of aerosols have the largest uncertainties in global climate predictions to quantify climate forcing due to man-made changes in the composition of the atmosphere. A better understanding of the formation, composition and transformation of aerosols in the atmosphere is of critical importance to better quantify these effects. Consequently, quantification of this variability requires comprehensive observations.

3.1. *Atmospheric aerosol monitoring*

Tropospheric aerosols are short-lived as a result their properties show high variability in space and time. To examine aerosol impact on the regional and global climate in addition to understanding and modelling the impact of aerosol on radiation budget and precipitation efficiency, a denser network of surface observatories located in different geographic regions is required. The IMD was perhaps the first institution in India to start systematic long-term measurement of aerosol optical properties. Determination of Angstrom's turbidity coefficient and Schuepp's turbidity coefficient from spectral direct solar radiation measured using broad band optical filters OG1, RG2 and RG8 started in 1957 at a number of stations in India (Chacko and Desikan, 1965; Mani and Chacko, 1963a). Angstrom's turbidity coefficient refers to wavelength of 1.0 μm and Schuepp's turbidity coefficient to the wavelength 0.5 μm. Later, turbidity coefficient measurement using Volz Sun-photometer started at 14 locations in India. Mani *et al*. (1969) found that north and central India during summer are highly turbid compared to rest of the country. They also found low values of wavelength exponent indicating predominance of the dust during summer months in north and central parts of India. Even though, aerosol properties are measured by different institutions at many sites in continuous and campaign modes, still there exists challenge in adequately characterizing the nature and occurrence of atmospheric aerosols and in including their effects in models to reduce uncertainties in climate prediction. The heterogeneity in aerosol optical and microphysical properties varies substantially in spatial and temporal scales over Indian subcontinent. Satellite-based remote sensing for monitoring aerosol properties is indispensable but not adequate component to acquire sufficient information base upon which advancement in understanding the role of aerosols in estimation of global climate change can be built.

Significant increase in atmospheric turbidity has been reported by several authors (Mani *et al*., 1977; Nand and Maske, 1983; Srivastava *et al*., 1992; Soni and Kannan, 2003). The observed atmospheric turbidity values at all the Indian GAW stations showed systematic seasonal as well as long-term variation apart from random fluctuations. However, the nature of variation is station dependent. Annual mean values of the turbidity coefficients showed a general increase of turbidity at all stations except Kodaikanal. The increasing trend of the turbidity at short wavelength (500 nm) indicates that it is caused more by fine size range aerosol, which are the product of primary and secondary production processes associated with anthropogenic activities. On an annual basis, the lowest turbidity was observed at Kodaikanal and Srinagar and highest in the north and central India. Volcanic eruptions across the globe in tropical latitudes have shown increased turbidity over the Indian region. Soni and Kannan (2003) and Singh *et al*. (1997) have reported a seasonal scale anomaly to the extent of 10-15% increase from mean values.

Aerosols, tiny particles suspended in the atmosphere, significantly influence climate, weather patterns, air quality, and public health. IMD established ground-based network for monitoring aerosol optical and physical properties using advanced instruments such as Aethalometers (for black carbon measurement), Nephelometers (for scattering coefficient measurements) and Sky Radiometers (for aerosol optical properties). The established network and the studies conducted so far have yielded new insights as presented below:

3.1.1. *Aerosol optical properties monitoring: Sky radiometer network*

The Skynet-India network, established by IMD (Fig. 5a), uses advanced sky-radiometers to measure solar direct and diffuse irradiances, enabling detailed analysis of aerosol properties. It provides critical data for improving climate models and understanding aerosol impacts. The sky-radiometer (models POM-01 and POM-02; make Prede, Tokyo, Japan) measures solar direct and diffuse irradiances in ultraviolet, visible and near-infrared wavelengths and these measurements are used for deriving aerosol optical properties *i.e*. spectral aerosol optical depth, single scattering albedo, normalized phase function or asymmetry parameter (g) and physical volume size distribution (Nakajima *et al*., 2007, 2020). The AOD is highly variable in space and time over India. The presence of north south gradient of AOD can be seen in all the months (Sateesh *et al*., 2018b). The Indo-Gangetic Plain (IGP) experiences large aerosol load because of diverse emission sources, local and long-range transported dust, regional meteorology and distinctive topography. Within IGP also major cities show high aerosol load mainly contributed by vehicular emissions. The mega city Delhi shows higher AOD compared to Rohtak despite of the close proximity and similar meteorological conditions (Mor *et al*., 2017; Taneja *et al*., 2017). A large variation in AOD from 0.23 to 1.89 with mean value 0.82 ± 0.31 is observed at Varanasi, indicating a highly variable aerosol load with significant heterogeneity in aerosol sources, types and properties (Tiwari *et al*., 2018). Short term extreme air pollution events mainly dominated by aerosols and caused by emissions from dust storms, stubble burning, festival celebrations such as Diwali and Holi are commonly experienced over Indian region (Kanawade *et al*., 2020; Kulkarni *et al*., 2020; Sateesh *et al*., 2018a; Soni *et al*., 2018; Srivastava *et al*., 2014a). The volcanic eruptions depending on their magnitude can bring long term changes in atmospheric aerosol loading affecting solar radiation and surface temperature at local and global scale (Soni *et al*., 2006; Soni and Kannan, 2003).

Diurnal and seasonal variations of radiative properties of aerosols have been monitored during 2006-2007 in New

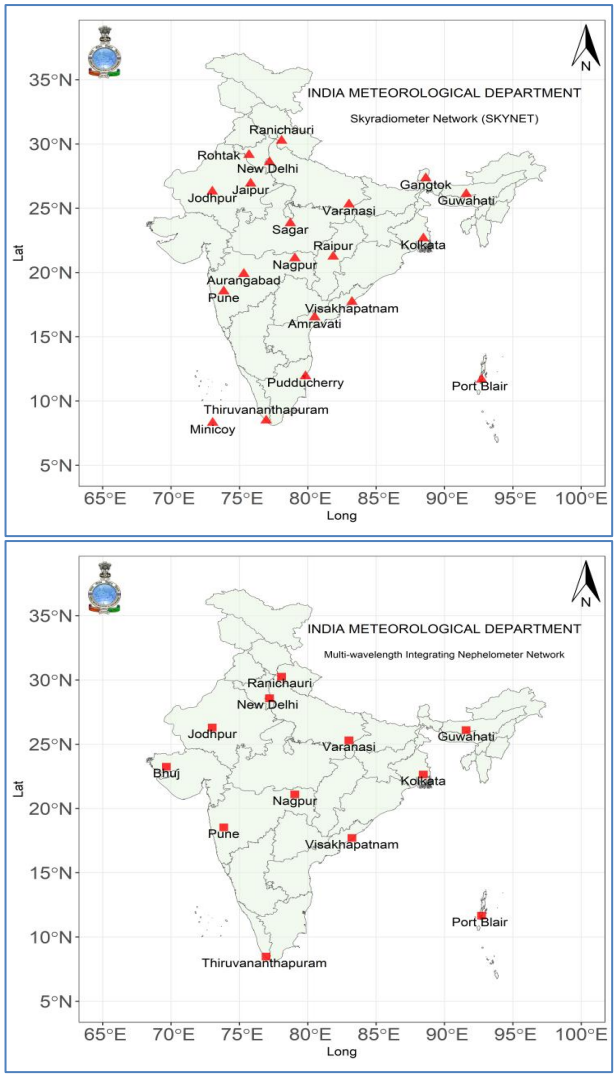

Fig. 5. IMD network for **(a)** Skyradiometer (SKYNET), **(b)** Multi-wavelength Integrating Nephelometers

Delhi using Sky-radiometer (POM-I) operating at wavelengths 315, 400, 500, 675, 870, 940 and 1020 nm. The results indicate that Aerosol Optical Depth (AOD) remains lowest at all wavelengths during Monsoon season while high values of Single Scattering Albedo (SSA) and Alpha (α) represent the presence of small aerosols and washout effect of large aerosols by rains. In Pre-monsoon season, AOD was found as second minimum with SSA and AOD lower than Monsoon season. However, AOD was lower in winter season as compared to post-monsoon season because of movement of westerly systems. Measurements have also shown that AOD values were higher at shorter wavelengths in comparison to the values at longer wavelengths for all four seasons of the year.

The Fig. 6 depicts the monthly variation of Direct Aerosol Radiative Forcing (DARF) at the surface (SFC), top of the atmosphere (TOA) and within the atmosphere

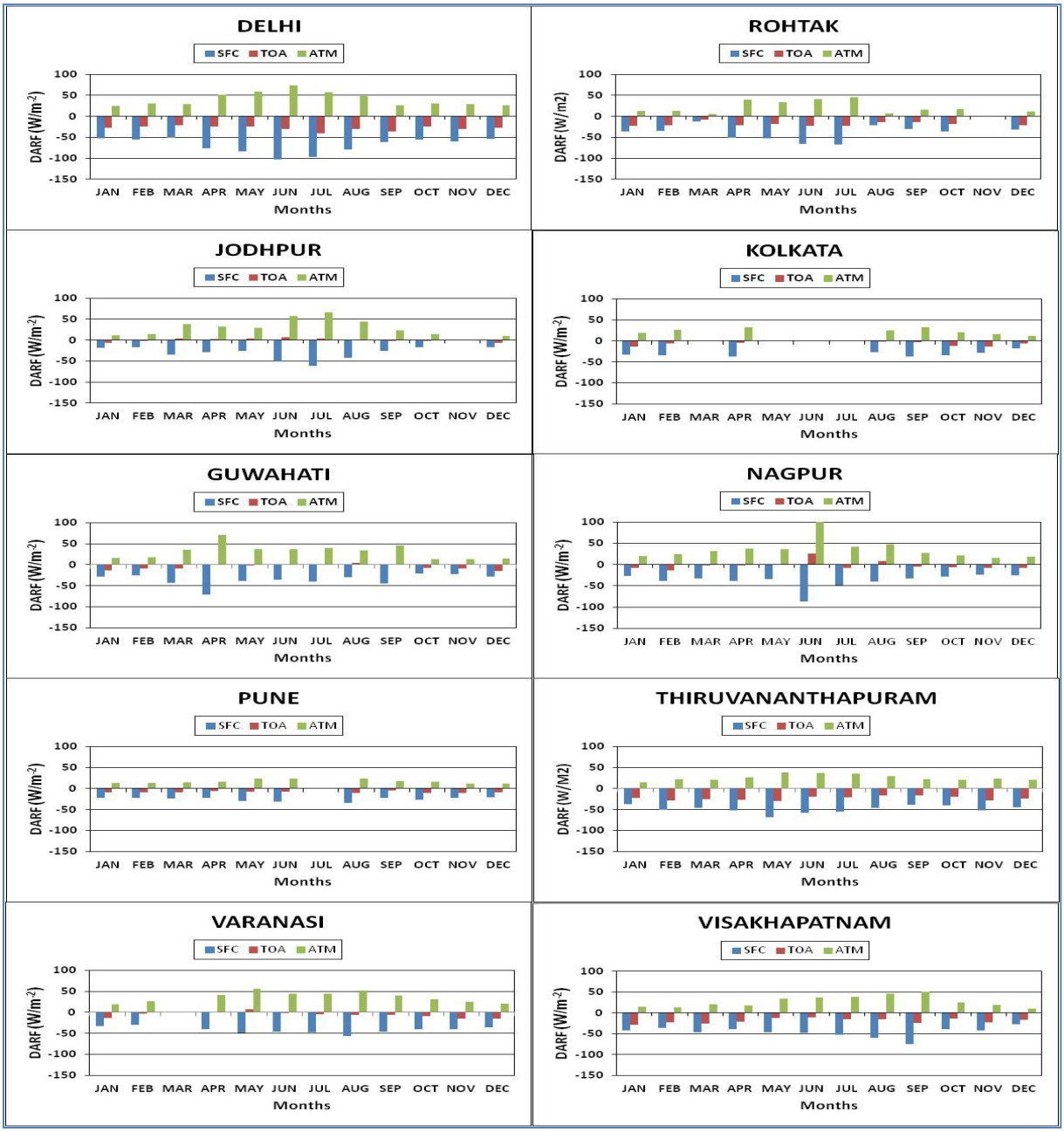

Fig. 6. Monthly variation of Direct Aerosol Radiative Forcing (DARF) over Skynet-India Stations of IMD (2012-2015)

(ATM) over selected Skynet-India stations monitored by IMD. DARF quantifies the influence of aerosols on the Earth's radiative energy balance, where negative values at the surface indicate a cooling effect due to reduced solar radiation reaching the ground, while positive values in the atmosphere signify heating caused by aerosol absorption. At stations like Delhi, Rohtak and Jodhpur, significant surface cooling is observed throughout the year, with peak negative forcing during summer months, attributed to high aerosol loading and enhanced scattering effects. Simultaneously, these stations exhibit positive atmospheric forcing, indicating localized heating due to aerosol absorption of solar radiation. The top-of-atmosphere (TOA) forcing at these locations fluctuates between slight positive and negative values, suggesting a near-neutral net radiative impact. In contrast, eastern stations such as Kolkata and Guwahati display moderate surface cooling and consistent atmospheric heating, reflecting the combined effects of local emissions and transported aerosols. Similarly, central and southern stations, including Nagpur, Pune and Thiruvananthapuram, exhibit relatively stable forcing patterns, characterized by moderate cooling

at the surface and atmospheric heating that follows seasonal trends. Coastal and southern regions generally show lower aerosol radiative forcing, likely due to cleaner atmospheric conditions and sea breeze influences. Northern stations like Varanasi and industrial regions such as Visakhapatnam exhibit strong surface cooling, with atmospheric heating effects increasing during specific months, indicating variability driven by seasonal emissions and meteorological factors. Seasonal trends reveal enhanced surface cooling during winter months (December-February), particularly over northern regions, due to increased aerosol concentrations and stable atmospheric conditions. In summer and monsoon months (June-September), the cooling effect intensifies in northern and central regions due to elevated aerosol optical depth, while atmospheric heating peaks in urban and industrial zones. The analysis highlights the spatial and temporal heterogeneity of aerosol radiative forcing across India. Northern and urban regions experience the strongest radiative forcing effects, driven by higher aerosol loading and complex atmospheric interactions. In contrast, southern and coastal stations show more moderate patterns, underscoring the influence of local sources, regional meteorology and aerosol composition on radiative forcing dynamics. These findings emphasize the critical role of aerosols in modulating regional climate and energy balance.

3.1.2. *Multi-wavelength integrating nephelometer network*

The Integrating Nephelometer is a type of instrument that measures the aerosol light scattering. It measures aerosol optical scattering properties by detecting (with a wide angular integration from 9º to 170°) the light scattered by the aerosol (Charlson *et al*., 1969; Heintzenberg and Charlson, 1996). Integrating nephelometers are widely used for monitoring and research applications related to air pollution and climate.

The Ecotech Aurora 3000 Integrating Nephelometer (Chamberlain-Ward and Sharp, 2011) uses an innovative LED light source to simultaneously measure light scattering at three wavelengths: 525 nm (green), 450 nm (blue) and 635 nm (red). This provides a wide and in-depth analysis of the interaction between light and aerosols. The Aurora 3000 includes backscatter measurement that allows both standards integrating measurements of 9° - 170° and also the back scatter 90° - 170°.

The Nephelometer are installed at 12 locations throughout the country (Fig. 5b) that measures, continuously and in real-time, light scattering in a sample of ambient air due to the presence of particulate matter (specifically, the scattering coefficient σ_{sp}) at three wavelengths. These measurements are combined with backscatter measurements that only sample 90° - 170°, allowing a more in-depth analysis of particle scattering. Forward scatter can be calculated by subtracting backscatter from total scatter. The measured values are adjusted automatically and in real-time by on-board temperature and pressure sensors. Aurora 3000 measures light scattering at three separate wavelengths simultaneously (525 nm (green), 450 nm (blue) and 635 nm (red)). Aerosol particles in the atmosphere directly influence the Earth's radiative balance by absorbing and scattering solar radiation, and indirectly by changing the microphysical properties of clouds. The amount of sunlight reaching the Earth's surface rather than scattered back to space is an important parameter for accurately modeling the influence of aerosol scattering on the Earth's radiative balance.

The Conditional Probability Function (CPF) at the 75^{th} percentile for 450 nm scattering coefficients shows a maximum probability of 0.35 (Fig. 7) for pollutants originating from the northwestern direction overall, as noted by Squizzato and Masiol (2015). However, seasonal variations exhibit very low probabilities with mixed patterns during the monsoon and pre-monsoon seasons, while the post-monsoon and winter seasons display a prominent peak in probability, reaching 0.421 (Fig. 7) from both the northwestern and southeastern directions. CPF probability for 525 nm indicates pollutant sources from the northwestern direction, with probabilities ranging between 0.15 and 0.30 overall (Fig. 7). Seasonal variations reveal contributions from both the northwestern and southwestern directions, with the probability during the study period peaking at 0.421. For 635 nm, the CPF probability of scattering coefficients ranges from 0.15 to 0.35 from the northwestern direction overall. During the post-monsoon and winter seasons, the probability peaks at 0.421 from the northwestern direction. In the pre-monsoon season, the CPF probability reaches 0.3, likely influenced by dust storms from the same direction. At all three wavelengths (450 nm, 525 nm, and 635 nm), pollutant probabilities consistently show dominance from the northwestern direction during the post-monsoon and winter seasons (Fig. 7).

3.1.3. *Black carbon monitoring network*

Initiated in 2016, the Black Carbon (BC) Monitoring Network initially consisted of 16 aethalometers (AE-33 Model, Magee Scientific) installed nationwide which was further augmented (Fig. 8). This initiative focuses on understanding BC distribution, sources, and impacts. Aethalometer works on light wavelength-dependence on absorption principle using suitable mass absorption cross – section values (Petzold *et al*., 2013). It uses seven

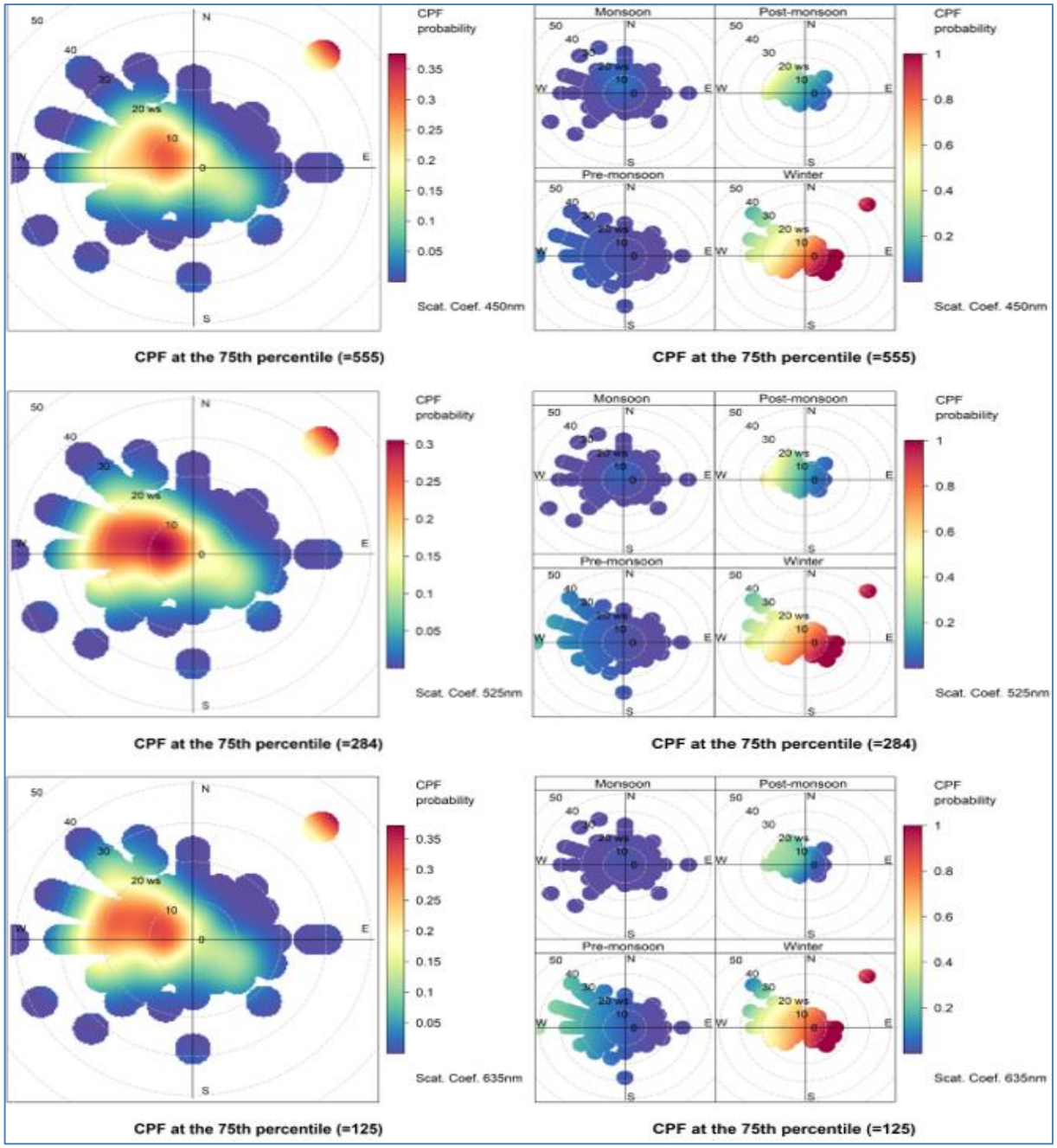

Fig. 7: Overall and Seasonal Conditional Probability Function (CPF) plot for scattering coefficients at New Delhi 2017

wavelengths (370, 470, 520, 590, 660, 880 and 950 nm) that allow spectral analysis for different purposes, such as mineral dust detection and source apportionment (Drinovec *et al*., 2015). It measures black carbon (BC) mass concentration (μgm^{-3}) and biomass burning (BB, in percent) black carbon, produced primarily from the incomplete combustion of fossil fuels, biomass, and other organic matter, is a significant pollutant with far-reaching environmental and health implications. These aerosols absorb solar radiation over a wide spectral band from UV to IR and contribute to the atmospheric warming (Bond *et al*., 2013; Bond and Bergstrom, 2006; Jacobson, 2001; Ramanathan and Carmichael, 2008). The global mean radiative forcing of BC aerosol formed due to fossil fuel and biofuel burning has increased from +0.20 Wm^{-2} to +0.40 Wm^{-2} (Myhre *et al*., 2013). BC aerosols act to increase lower tropospheric heating and reduce the amount of solar radiation reaching the surface.

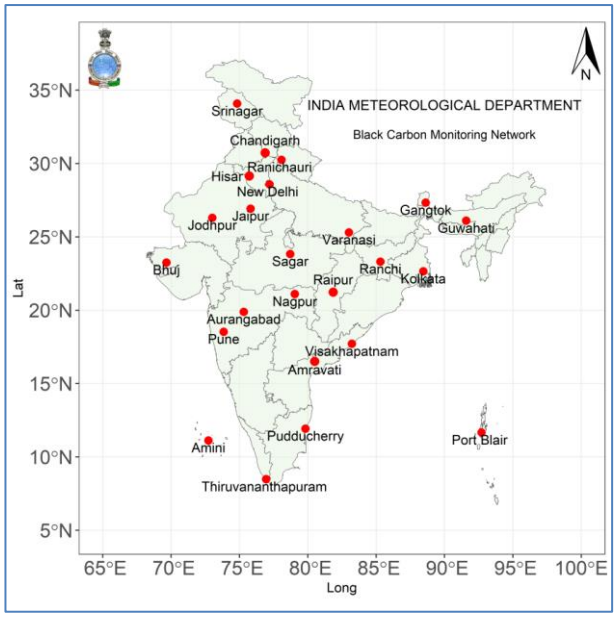

Fig. 8. IMD Black Carbon Aerosol monitoring network

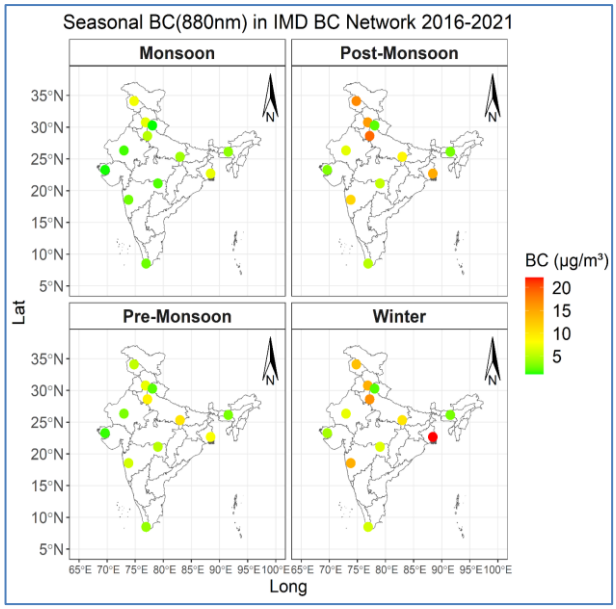

Fig. 9. Long term seasonal mean variation of BC over India during 2016-2021

Indo-Gangetic plain is a densely populated region of India and is termed a hotspot for BC emissions (Ramanathan and Carmichael, 2008). Improved understanding in characteristics and spatial heterogeneity of BC aerosols over India and in particular Indo-Gangetic Plain would provide valuable information for guiding measures to reduce emissions and to air pollution and climate change in the region. An analysis of the absorption characteristics and source apportionment of BC in western India was conducted by Sateesh *et al*. (2019). The heterogeneity in spatial distribution of the BC aerosol over India was studied by Kumar *et al*. (2020). Long-term trends and variability in BC concentrations were examined by Kumar *et al*. (2023), revealing an overall declining trend in BC concentrations across India. The Fig. 9 illustrates the seasonal and spatial variability of black carbon (BC) aerosol concentrations (measured at 880 nm) across the BC aerosol network of IMD for the period 2016-2021. The data is presented for four seasons: Monsoon, Post-Monsoon, Pre-Monsoon and Winter, with BC concentrations represented by a color gradient from green (low concentrations, ~5 µg/m³) to red (high concentrations, ~20 µg/m³). Seasonal patterns reveal distinct variations, with lower BC levels during the Monsoon season, likely due to wet deposition by rainfall, and higher concentrations in Winter, particularly in northern India, attributed to increased biomass burning, reduced boundary layer height, and stable atmospheric conditions. The Post-Monsoon and Pre-Monsoon seasons show moderate to high BC concentrations, driven by factors such as agricultural residue burning, industrial emissions and dry weather. Spatially, northern India consistently exhibits higher BC levels across seasons, which can be linked to dense population, intense anthropogenic activities and the impact of agricultural practices in the Indo-Gangetic Plain, while southern and coastal regions report lower concentrations due to better ventilation and fewer emission sources. These findings highlight the significant role of BC aerosols in air quality degradation, particularly in northern India, where severe pollution episodes during Winter and Post-Monsoon seasons have serious implications for public health and visibility. The role of BC aerosol as a climate forcer, with its ability to absorb solar radiation, contributes to atmospheric heating, alterations in monsoonal patterns, and accelerated glacier melting in the Himalayas. Further studies are currently underway to investigate the impact of BC on monsoon breaks, heatwaves, and fog formation.

The BC aerosol network plays a crucial role in addressing air pollution and climate change challenges. By providing data on black carbon distribution and sources, it helps policymakers design targeted mitigation measures. Additionally, it enhances understanding the role of black carbon in regional climate phenomena like monsoons and glacier retreat. The initiative supports India's broader goals of improving air quality, reducing carbon emissions, and contributing to global efforts to combat climate change.

3.2. *Estimates of indirect radiative impacts of aerosols over India*

Although, observations of aerosols have been ongoing over Indian region since long (Parameswaran *et al*., 1984; Devara *et al*., 1986), the attempts for quantitative estimates of radiative forcing of aerosols have begun by the end of 1990's. Such initial attempts are dated back to pre-Indian

Ocean experiment (INDOEX) observations in 1996. Jayaraman *et al*. (1998) had used a slope method (between radiation and aerosol optical depth for different zenith angles) and found reduction of 42 Wm-2 of radiation for every 0.1 increase in aerosol optical depth during pre-INDOEX experiments. Using a combined observation and modeling approach, Satheesh *et al*. (1999) estimated a reduction of 50 to 80 Wm-2 of radiation at the surface during INDOEX. The introduction of user friendly optical models and radiative transfer models has improved the estimation of direct radiative impacts over Indian region. Optical Properties of Aerosols and clouds (OPAC) (Hess *et al*., 1998) was one of the optical models, which have been popularly used over Indian region. This model provides the essential aerosol optical parameters such as AOD, SSA and asymmetry parameter (ASP), which are necessary for forcing estimation using chemistry data sets. Hence it became easy that one can obtain these optical parameters much simply along with chemistry observations than using sophisticated optical sun/sky scanning instruments. The Santa Barbara Discrete ordinate atmospheric radiative transfer (SBDRAT) (Ricchiazzi *et al*., 1998) is one of the most popular radiative transfer models being used in India for the estimation of radiative forcing. OPAC model in conjunction with SBDART has provided the estimates of radiative forcing over different Indian terrains. The radiative forcings are typically estimated for the short wave spectrum of solar radiation (0.3-3μm) at the surface and Top of the Atmosphere (TOA), the difference of which yields the net atmospheric absorption by aerosols. Vinoj *et al*. (2004) using a combination of OPAC and SBDART has shown a reduction of solar radiation by 15 to 24 Wm-2 over Bay of Bengal. Further several studies used this combination of models for estimating forcing over different Indian regions (*eg*., Babu *et al*., 2002; Panicker *et al*., 2010; Srivastava *et al*., 2014 *etc*.).

The uncertainty in aerosol direct forcing estimates has been further reduced with the establishment of network-based observations and usage of more accurate instruments such as sun/sky radiometers. Using sun/sky radiometer data along with SBADRT model, Pandithurai *et al*. (2004) has quantitatively estimated the aerosol radiative forcing over Pune. The results showed a reduction of solar radiation by 33 Wm^{-2} at the surface, 0 at the Top of the atmosphere (TOA), yielding an aerosol atmospheric absorption of 33 Wm^{-2} over the region. The trend over Delhi was found to be much higher, where an enhanced atmospheric absorption up to 22 Wm^{-2} was observed in winter months (Pandithurai *et al*., 2008). Table 4 depicts detailed results of radiative forcing estimates over different regions in Indian sub-continent.

Species segregated impact of aerosols on climate (especially for carbonaceous aerosols) also has been estimated over Indian region. Organic carbon (OC), elemental carbon (EC) and Black carbon (BC) are three major identified climate forcing aerosols. While, OC in general is a scattering species, BC and EC are strong absorbents of radiation. Studies have shown that even though BC contribution is less than 6% of total aerosol mass, it contributes 55-75% of total aerosol absorption (Panicker *et al*., 2010b; Sreekanth *et al*., 2007). Also in the chemical composition, OC was found to have much larger contribution by mass compared to EC. However, it is found that EC contributes up to 10 times larger atmospheric warming compared to OC, in spite of its meager presence due to strong absorption efficiency (Panicker *et al*., 2019, 2018). While, the aerosol forcing estimations were mainly concentrated in the shortwave, long wave forcing had generally been ignored. However it is found that the aerosol long wave forcing at the surface, neutralizes the forcing by up to 8% (Panicker *et al*., 2008) and is an important component of forcing estimates.

The establishment of federated observational networks (AERONET and SKYNET) has considerably reduced the uncertainty level in aerosol direct forcing across the world. However, the uncertainty remains high in the indirect radiative forcing estimation. The uncertainty persists because of the lack of simultaneous observations of aerosols and cloud microphysical parameters in different regions. Aerosol Indirect effect (AIE) is typically predicted to range between 0 to 0.33. However, negative values of AIE also has been reported over Indian region, attributed due to the source regions and hygroscopicity of aerosols. Tripathi *et al*. (2007) have carried out an experiment to determine AIE over Indo Gangetic plain and found a significant positive AIE in 37-68% area for water clouds and 35-53% for ice clouds. Abish and Mohanakumar (2011) also observed a significant AIE over northern India. Panicker *et al*., (2010a) using MODIS satellite observations has quantitatively estimated the indirect effect over different regions in India. It is found that AIE values ranges between -0.53 to 0.45 for ice clouds and -0.55 to 0.52 for water clouds and plays pivotal role in contrasting monsoon seasons. The negative values of AIE were attributed to the enhanced presence of hygroscopic aerosols. The Cloud aerosol interaction and precipitation enhancement experiment (CAIPEEX) has been a major attempt to unravel the complex aerosol-cloud interactions over Indian region. The aircraft based CAIPEEX has measured all the essential aerosol-cloud microphysical parameters to estimate the indirect effect of aerosols (Kulkarni *et al*., 2012). Pandithurai *et al*. (2012) has shown that the spectral dispersion effect offsets the AIE by 39% (estimated AIE 0.07 to 0.13). Dipu *et al*. (2013) has studied how elevated aerosol layer impacts cloud macrophysics. Several CAIPEEX results have provided insight towards the influence of cloud condensation nuclei (CCN) in

TABLE 4

Direct aerosol radiative forcing estimates (in Wm^{-2}) over different Indian regions

Location	DRF (Wm^{-2})			Reference
	SFC	TOA	ATM	
Pune	-33	0	33	Pandithurai *et al*. (2004)
	-19.5 to -38.7	-1.7 to -5.6	14.3 to 35.4	Bhaskar *et al*. (2017)
Delhi	-39 to -99	27 to 123	63 to 222	Pandithurai *et al*. (2008)
Varanasi	-38.6 to -76	-5.3 to +5.8	33.2 to 81.8	Tiwari *et al*. (2018)
Bangalore	-23	5	28	Babu *et al*. (2002)
Manora Peak	-3 to -50	-2 to +14	3 to 65	Srivastava *et al*., (2014b)
Trivandrum	-47.8 to -56.1	1.8 to 4.1	46 to 52	Suresh Babu *et al*. (2007)
Nainital	-4.2	0.7	4.9	Pant *et al*. (2006)
Ranichauri	-26.9	-10.9	16	Nair *et al*. (2017)
Jaipur	-22.59 to -32.2	-5.6 to -11.4	14.04 to 22.47	Verma *et al*. (2017)
Kanpur	-43	-13	30	Dey and Tripathi (2007)
Dibrugarh	-37.1	-1.4	35.7	Pathak *et al*. (2010)
Ahmedabad	-45 to -56	0 to 4	45 to 60	Ramachandran and Kedia (2010)
Rohtak	-20 to -34	-13 to -16	7 to 12	Mor *et al*. (2017)
Patiala	-30 to 96.7	-19.4 to 0.04	30 to 77	Singh *et al*. (2016)
Dehradun	-53.29	-14.49	38.8	Patel and Kumar (2015)
Jodhpur	-24.06 to -44.15	-3.65 to -7.79	17.46 to 40.50	Bhaskar *et al*. (2015)

TABLE 5

Aerosol Indirect effect (AIE) estimates over different Indian regions

Location	**AIE**	**Source**	**Reference**
Different Indian regions	-0.53 to 0.45 (for Ice clouds) -0.55 to 0.52 (for water clouds)	MODIS satellite	Panicker *et al*., (2010a)
Central/South India	-0.8 to 0.8	MODIS satellite	Manoj *et al*. (2012)
North-East India	0.32-0.48 (for BC)	CAIPEEX	Panicker *et al*. (2016)
Mahabubnagar	0.01 – 0.23	CAIPEEX	Harikishan *et al*. (2016)
Mahabaleshwar	0.05-0.088	HACPL	Anil Kumar *et al*. (2016)
Mahabaleshwar	0.01-0.13	HACPL	Ansari *et al*. (2020)

modulating cloud microphysics (Padmakumari *et al*., 2017; Prabha *et al*., 2012 *etc*.). While several studies have estimated the AIE values, converting it to exact radiative forcing remains a challenge. Panicker *et al*. (2016) has made an attempt to quantitatively estimate the forcing arising due to indirect effect. The estimated BC- AIE was found to induce a reduction of radiation by 37 Wm^{-2} at the surface and TOA forcing values were found to be up to +14.8 Wm^{-2}. Table 5 depicts Aerosol Indirect effect estimates over different regions in Indian sub-continent.

4. Solar irradiance monitoring over India

The Sun is the dominant source of energy for the Earth's climate system (Kren *et al*., 2017) yet the full influence of solar variability on climate remains quantitatively incomplete. Solar forcing influences combined with other natural variabilities are complex in both magnitude and phase. Broadly, the climate variations originate from variations of the radiative balance at the top of atmosphere. India is having a long history of radiation measurement, dating back to November 1879, when the first radiation measurements were made in Kolkata, though the instrument details not clearly indicated. During 1883-1887, radiation measurements were recorded at Mussoorie, followed by Kodaikanal in 1895. More systematic measurements began in 1930 at Pune, where an Ångström pyrgeometer was used for nocturnal radiation measurements and an Ångström pyrheliometer was employed to measure direct solar irradiance.

A significant expansion in solar radiation monitoring occurred during the International Geophysical Year (1957–58), when the India Meteorological Department (IMD) established four radiation stations in Pune, New Delhi, Kolkata, and Chennai. These stations initially measured global and diffuse solar irradiance (using MG pyranometers), direct solar irradiance (using Ångström pyrheliometers with three broadband filters), and nocturnal net terrestrial radiant energy (using Ångström pyrgeometers). By 1976, the IMD network had expanded to include 31 operational stations, and by 1986, 14 additional stations were added. IMD radiation network now comprises 45 stations and includes UV-A and UV-B radiation measurements. In 2011, the Ministry of New and Renewable Energy (MNRE) initiated the Solar Radiation Resource Assessment (SRRA) project and established 115 automatic meteorological stations, equipped with state-of-the-art instruments to measure direct, diffuse, and global irradiance. The SRRA aimed to assess and quantify solar radiation, process data, ensure quality and model radiation for the development of a solar atlas of India.

The World Meteorological Organization (WMO) has designated the Central Radiation Laboratory at IMD Pune as one of two Regional Radiation Centers for Asia, the other being in Tokyo. The Central Radiation Laboratory at Pune is equipped with a hierarchy of standard instruments-primary, secondary, transfer, working, and travelling standards to ensure measurement accuracy. The laboratory adheres to the World Radiometric Reference (WRR) for data generation, and one primary instrument regularly participates in the International Pyrheliometer Comparisons, held every five years at the World Radiation Centre, Davos, Switzerland. The accuracy of field instruments in the IMD network is summarized in Table 6.

TABLE 6

Accuracy of field instruments in the IMD network.

Instrument	Accuracy Specified by WMO	Accuracy Permitted by IMD
Ångström Pyrheliometer	± 0.5%	± 0.5%
Thermoelectric Pyrheliometer	± 1.0%	± 1.0%
Thermoelectric Pyranometer	± 3.0%	± 2.0%
Bimetallic Pyranograph	±5.0%	±5.0%
Net Pyrradiometer	±7.0%	± 5.0%
Ångström Pyrgeometer	± 1.0%	

The first measurements of total radiation from the Sun and sky in India, conducted in Pune in 1935, were published by Raman (1938). Early studies, constrained by a lack of a radiation network, estimated surface solar radiation using sunshine duration and meteorological parameters (Ramdas and Yegnanarayanan, 1956; Mani *et al*., 1962b; Yadav, 1965). Mani *et al*. (1962b) conducted one of the earliest comprehensive studies, analyzing sunshine duration and surface solar radiation across 15 Indian stations and finding good agreement between observed and estimated values in major cities. Subsequent research explored seasonal and diurnal variations (Mani *et al*., 1962a), cloud transmission effects (Mooley and Raghavan, 1963) and diffuse radiation (Mani and Chacko, 1963b; Desikan *et al*., 1969). Mani *et al*. (1967) prepared radiation maps over the Indian Ocean, highlighting radiation minima in equatorial and monsoon regions and maxima in high-pressure zones. High urban pollution was linked to increased diffuse radiation (Desikan *et al*., 1969). Mani (1971) analyzed global radiation balance using satellite data, showing good agreement with ground and airborne measurements. High-altitude studies (Mani *et al*., 1977) attributed low direct solar radiation to dust layers during pre-monsoon months. Comprehensive works, such as Handbook of Solar Radiation Data for India (1980) (Mani, 1981) and Solar Radiation Over India (1982) (Mani and Rangarajan, 1982), are considered reference material for meteorologists and energy experts. Recent studies address long-term variability, trends and pollution effects on radiative fluxes (Desikan *et al*., 1994b, 1994a; Padmakumari *et al*., 2017b; Soni *et al*., 2016, 2012).

India experiences significant levels of global solar radiation annually, with distinct spatial and temporal variations influenced by geography, weather conditions, and seasonal changes. India receives high solar irradiance annually at the surface ranging roughly from 1700 to 2200 $kWhm^{-2}$ depending on geographical location (Mani and Rangarajan, 1982; Soni *et al*., 2012). Annual bright sunshine duration ranges from 2,000 to 3,200 hours, depending on the location. The peninsular region receives an average of 230 Wm^{-2}, while the Rann of Kutch records the highest annual solar radiation exposure, exceeding 250 Wm^{-2} (8,000 MJm^{-2} annually). Long-term observations indicate variation in annual global irradiance, from 189 Wm^{-2} in Kolkata to 229 Wm^{-2} in Jodhpur.

Seasonal changes in solar irradiance are distinct across India. In January, the northern plains receive approximately 175 Wm^{-2} or less due to low solar elevations, shorter daylight hours, and weather conditions like fog and smog. The Kashmir Valley experiences the lowest irradiance at less than 60 Wm^{-2}, whereas the Deccan Plateau receives nearly 230 Wm^{-2}. By April and May, irradiance rises significantly to over 230 Wm^{-2} across most regions, with Saurashtra and Rajasthan receiving more than 280 Wm^{-2}. During the monsoon season, global irradiance decreases significantly due to cloud cover, although Northwest India and Kashmir continue to receive over 220 Wm^{-2}, while areas like the Andaman Islands and

Lakshadweep receive around 160 Wm^{-2} and 185 Wm^{-2}, respectively. Post-monsoon months, such as October, show relatively uniform irradiance ranging from 170 to 220 Wm^{-2}, except for the Kashmir Valley, where levels drop below 160 Wm^{-2}. During November and December, irradiance in southern states, particularly South Andhra Pradesh and Tamil Nadu, decreases further to below 175 Wm^{-2} due to the northeast monsoon.

Diffuse radiation, which constitutes a significant portion of global solar radiation, also shows spatial and seasonal variations. Annual diffuse radiation under all-sky conditions ranges from 80 to 100 Wm^{-2}, with an average of approximately 90 Wm^{-2}. Coastal regions generally record higher diffuse radiation due to increased cloud cover, with values often exceeding 90 Wm^{-2}. During winter months (December-January), when cloudiness is minimal, diffuse radiation levels drop to 45-60 Wm^{-2}, constituting less than 30% of global radiation in most areas. However, during the monsoon season, diffuse radiation increases significantly to over 115 Wm^{-2}, accounting for more than 70% of global irradiance in many regions. Post-monsoon months see a sharp decline in diffuse radiation to 70-80 Wm^{-2} across most locations. Under clear skies, diffuse radiation levels range between 56 and 72 Wm^{-2}, mainly due to atmospheric molecules and aerosols, making it a reliable indicator of aerosol pollution levels across the country.

Observational records from solar radiation network of IMD reveal significant multidecadal variations in incident solar irradiance and indicate a decline in solar radiation (dimming) (Padma Kumari *et al*., 2007; Soni *et al*., 2012), without clear signal of a turnaround of this trend (brightening) such as commonly seen in many other areas of the globe (Soni *et al*., 2016). The dimming signal over India is predominantly caused by increasing aerosol loading. With these recent changes in the solar irradiance, together with the foreseen strong growth in installed solar energy capacity, it is of utmost importance to investigate the future evolution of solar radiation conditions induced by anthropogenic climate change over Indian region. The turbidity coefficient is a critical parameter representing the attenuation of solar radiation due to atmospheric aerosols, water vapor, and other particulates. An increasing turbidity coefficient indicates higher atmospheric pollution, reducing the clarity of the atmosphere and altering solar radiation's direct and diffuse components. Most Indian cities analyzed for solar irradiance trends exhibit an increasing turbidity coefficient over the long-term period (1971-2010), with some showing more prominent trends than others. Cities like Kolkata, Delhi, and Visakhapatnam demonstrate significant reductions in global irradiance and sunshine duration, which are consistent with elevated atmospheric turbidity levels. These reductions are linked to increasing aerosol concentrations from urbanization, industrial activities, and vehicular emissions. For instance, the diffuse irradiance trends in cities such as Nagpur (+2.2% per decade) and Chennai (+2.1% per decade) suggest a higher scattering effect caused by aerosols.

A long-term analysis (1971-2010) of global irradiance (G), diffuse irradiance (D), and daily sunshine duration (S) under all-sky conditions across Indian cities (Table 7) reveals notable spatial variations and trends. Global irradiance ranged from 191.0 Wm^{-2} in Shillong to 228.7 Wm^{-2} in Pune, while diffuse irradiance varied between 85.2 Wm^{-2} in Jodhpur and 101.1 Wm^{-2} in Trivandrum. Sunshine duration ranged from 5.7 hours in Shillong to 8.5 hours in Jodhpur. Statistically significant negative trends in global irradiance were observed in most locations, with declines of up to -4.1% per decade in Kolkata. Diffuse irradiance generally showed slight increases, with the largest positive trend of 2.2% per decade in Nagpur. Sunshine duration exhibited consistent declines, with significant reductions in cities like Delhi (-6.3% per decade) and Visakhapatnam (-5.7% per decade). These trends highlight the potential impact of atmospheric changes, such as increased aerosols and cloud cover, on solar radiation and sunshine availability.

Global irradiance derived from geostationary satellite imagery, on the other hand, have temporal resolution ranging from 5 min (GOES-17) to 1 h (Himawari-7) and offer a large geographical coverage but has relatively large uncertainties in GHI estimation mainly due to the spatial resolution of satellite and satellite-to-irradiance modelling uncertainties, especially in complex terrains (Ruiz-Arias *et al*., 2010) and at low sun heights (Bright, 2019). The Indian National Satellite (INSAT) series started the operation since 1990s. INSAT-3D/3DR/3DS missions in 2013, 2016 and 2024 provide half-hourly global irradiance at 4 km spatial resolution from visible channel radiance (Bhattacharya and Nigam, 2015; Vyas *et al*., 2016). Modern reanalysis products, such as the Modern Era Retrospective-analysis for Research and Applications (MERRA), offer advanced insights by isolating aerosol and cloud effects. Developed by NASA, MERRA uses the Goddard Earth Observing System (GOES) Data Assimilation System (DAS) to provide datasets from 1979 to the present. These datasets include net downward shortwave and long wave fluxes, sensible and latent heat fluxes, and ground heat fluxes. Detailed documentation is available on the MERRA website: http://gmao.gsfc.nasa.gov/MERRA. While reanalysis datasets address gaps left by observational networks, remote sensing has emerged as a vital tool for obtaining global radiation data with temporal continuity and spatial homogeneity. The widely used satellite products of radiation include the Surface Radiation Budget project (SRB), the Clouds and the Earth's Radiant Energy System (CERES) and the International Satellite

TABLE 7

Long-term mean values and trend analyses of global irradiance (G), diffuse irradiance (D) and daily bright sunshine duration (S) in India under all sky conditions for 1971-2010. Trend values in bold are statistically significant.

Station Name	Long-term Mean (Standard Deviation)			Trend (% per decade)		
	G (Wm^{-2})	D (Wm^{-2})	S (Hours)	G	D	S
Ahmedabad	226.2 (11.7)	87.6 (4.6)	8.2 (0.3)	**-3.3**	0.4	-1.3
Jodhpur	228.4 (12.1)	85.2 (5.2)	8.5(0.4)	**-3.6**	0.8	0.0
Delhi	216.2 (10.2)	93.4 (3.8)	7.5 (0.7)	**-3.4**	0.4	**-6.3**
Kolkata	191.4 (10.5)	95.5 (5.0)	6.1 (0.6)	**-4.1**	-0.4	**-3.5**
Chennai	224.8 (7.7)	98.4 (6.8)	7.4 (0.4)	**-1.7**	**2.1**	**-3.6**
Mumbai	215.4 (8.5)	92.7 (4.9)	7.3 (0.4)	**-2.4**	**1.6**	-0.4
Nagpur	214.6 (7.1)	88.1 (4.8)	7.5 (0.5)	**-2.0**	**2.2**	**-2.4**
Pune	228.7 (8.6)	88.6 (3.5)	7.8 (0.4)	**-1.5**	-1.4	**-2.5**
Panjim	228.3 (12.2)	95.7 (5.1)	7.6 (0.4)	**-2.0**	**1.7**	**-2.8**
Shillong	191.0 (8.6)	90.6 (3.7)	5.7 (0.3)	-0.1	0.5	**-2.4**
Trivandrum	226.1 (11.4)	101.1 (3.6)	6.3 (0.4)	**-3.4**	0.8	**-3.0**
Visakhapatnam	218.5 (10.8)	94.3 (5.3)	7.2 (0.6)	**-3.9**	1.0	**-5.7**

Cloud Climatology Project (ISCCP). The satellite missions, such CERES (Wielicki *et al*., 1996) and Solar Radiation and Climate Experiment (SORCE) (Anderson and Cahalan, 2005), have significantly improved knowledge of Earth's radiation budget, especially at the Top of the Atmosphere (TOA). These satellites enable high-accuracy determination of TOA radiative fluxes (Loeb *et al*., 2012). Unlike TOA fluxes, surface fluxes cannot be directly measured by satellites. While satellite-derived radiation data are sufficiently accurate at global scales, their regional-scale accuracy remains uncertain.

5. Air quality monitoring and forecasting

To protect citizens from unhealthy air, many countries have real-time air quality forecasting programs in place to forecast the concentrations of pollutants such as O_3, NO_2, CO, SO_2, $PM_{2.5}$, PM_{10}. The air quality early warning alerts allow pollution control authorities and people to take precautionary measures to reduce air pollution and avoid or limit their exposures. Accurate real-time air quality early warning system therefore offer tremendous societal and economic benefits by enabling advanced planning for individuals, organizations, and communities in order to reduce pollutant emissions and their adverse health impacts.

Starting in the 1970s, various air quality forecast techniques and tools which were largely based on empirical approaches and statistical models trained or fitted to historical air quality and meteorological data. These methods included multiple linear regression, nonlinear regression, neural networks *etc*. All such statistical methods rely on the close relation of air pollutant concentrations with a small set of meteorological and chemical predictors. The statistical guidance was then used as a first guess for "expert" analysis leading to the final forecast. The level of sophistication in models increased considerably to overcome some of the limitations and address non-linearity of the photochemical system during the 1990s. With significant advances in computational resources and development of sophisticated 3-D numerical air quality models (AQMs) on urban, regional, and global scales that account for meteorology, emissions, chemistry, and removal processes led to a significant leapfrog. The efforts to deploy 3D-AQMs first begun in Germany in 1994, Japan in 1996, Australia in 1997, and Canada in 1998 and then expanded in the U.S., other countries in Europe and China (Zhang *et al*., 2012). Learning from initial air quality forecast applications, more sophisticated techniques such as 4-dimensional variational method (4D-Var), Kalman-filtering and ensemble methods have been used in conjunction with 3D-AQMs to improve the accuracy. It is observed that the ensemble forecasts often, but not always, perform better than individual member forecasts and the weighting or bias correction approaches may improve performance.

The operational air quality forecast service is relatively recent in India compared to weather forecasting services. Recognizing the need for air quality forecast service during Commonwealth Games 2010, Ministry of Earth Sciences (MoES), Government of India, introduced the System of Air Quality Forecasting and Research (SAFAR) for Delhi to provide location specific information on air quality in near real time and its forecast 1-3 days in advance (Beig *et al*., 2013, 2015, 2021). The SAFAR was the first operational air quality forecast service

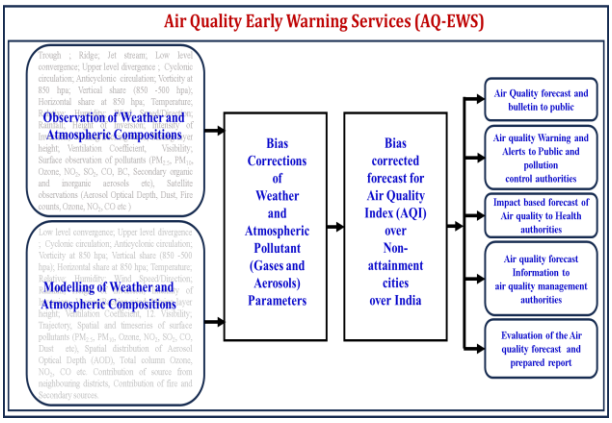

Fig. 10. Flow diagram of Air Quality Early Warning System.

introduced in India. The SAFAR was initiated by IITM, Pune in collaboration with IMD and National Centre for Medium-Range Weather Forecasting (NCMRWF) under the aegis of MoES. The Air Quality Monitoring and Forecasting services were extended to Pune in 2013, Mumbai in 2015 and Ahmedabad in 2017. Recognizing the huge cost of air pollution to society as well as the scientific advances to forecast and monitor air quality, Ministry of Earth Sciences further introduced Air Quality Early Warning System (AQEWS) in 2018 by bringing in more sophisticated modelling framework and observations for air quality forecast for all India level. The AQEWS is jointly developed by the scientists of IITM, Pune, IMD and NCMRWF. Now, the operational air quality forecast services are provided by IMD through AQEWS.

5.1. *Air quality early warning system (AQEWS)*

The Air Quality Early Warning System (AQEWS), launched in 2018 by the Ministry of Earth Sciences, represents a significant advancement in air quality forecasting with its sophisticated modeling framework and is widely used (Ghude *et al*., 2020; Govardhan *et al*., 2023; Jena *et al*., 2021; Kalita *et al*., 2023). AQEWS utilizes two primary models: WRF-Chem, an online coupled model that simultaneously generates meteorological and chemical forecasts, and SILAM, an offline coupled model that separates meteorological forecasting from the chemistry transport process. Key components of AQEWS include meteorological and chemistry transport models (either online or offline), emission models that project real-time emissions based on energy or fuel consumption, and meteorology-dependent emissions like biogenic, sea salt, and erodible dust emissions. Regional-scale models rely on initial and boundary conditions from General Circulation Models (GCMs) and Global Chemistry Transport Models (GCTMs). Operational steps in AQEWS involve initiating forecasts using chemical conditions from GCTMs or observations for the first day, with subsequent days using the previous day's output. Bias correction techniques further enhance accuracy by adjusting systematic biases based on prior forecasts and observations. Urban forecasting integrates detailed traffic emissions, urban meteorology, and regional background concentrations to produce accurate predictions.

The Air Quality Early Warning System (AQEWS) is designed to provide timely air quality forecasts and alerts to safeguard public health and guide decision-making. The flow chart (Fig.10) above illustrates the key components of the system:

(*i*) Near Real-Time Observations: A leapfrog in India's real-time air quality monitoring came with the Central Pollution Control Board (CPCB) developing a real-time data repository. This platform facilitates the communication of real-time air quality observations and AQI to the public via its web portal (https://app.cpcbccr.com). AQEWS incorporates continuous monitoring of air quality and meteorological parameters using automated monitoring systems. These real-time observations are critical for initializing forecasting models and validating outputs to ensure accuracy.

(*ii*). Multi-Model and Multi-Scale AQ Forecast: The system utilizes advanced forecasting tools, including multiple models (*e.g*., WRF-Chem, SILAM) at different scales (urban, regional, and national). These models integrate data on meteorology, emissions, and atmospheric chemistry to simulate pollutant dispersion, chemical transformations, and removal processes.

(*iii*). Air Quality Bulletin and Alerts: The forecasts are converted into user-friendly formats such as air quality bulletins and alerts. These include spatial and temporal distributions of pollutant concentrations and AQI values, which are disseminated to the public and authorities through web platforms, display boards, and mobile alerts.

6. Air quality modelling system

The AQEWS has evolvedan extensive air quality modelling program that develops, evaluates, and applies models to support a wide variety of air quality management needs. The AQEWS deployed two major air quality modelling systems WRF-Chem and SILAM.

6.1. *WRF-chem (MoES-UCAR joint activity): multi-scale air quality prediction system*

The multi-scale air quality prediction system integrates global, regional and city-scale setups to provide comprehensive air quality forecasts for Delhi, enhancing decision - making and mitigation strategies. The global

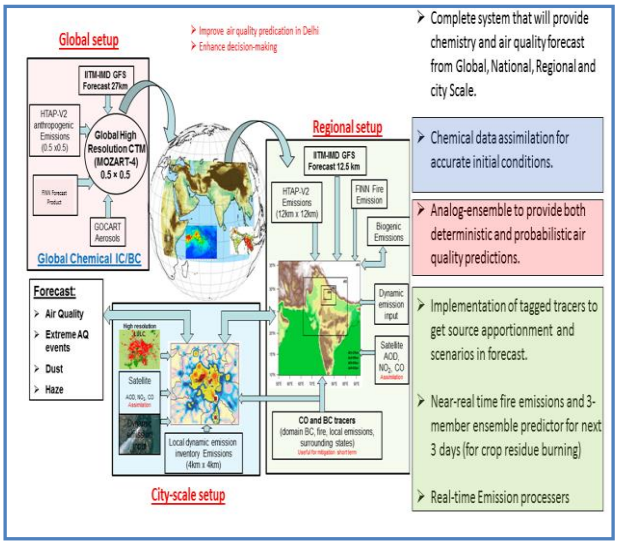

Fig. 11. Multi-scale air quality prediction system using WRF-Chem

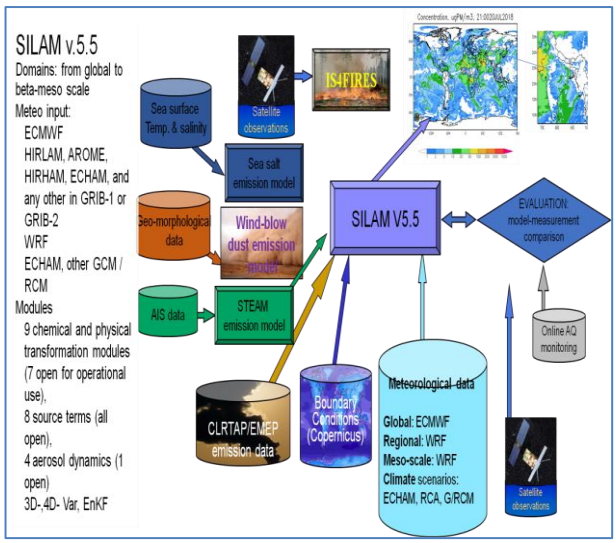

Fig. 12. Work flow chart of SILAM v5.5

setup utilizes HTAP-V2 anthropogenic emissions and the Global High-Resolution Chemical Transport Model (MOZART-4) at 0.5° x 0.5° resolution, alongside GOCART aerosols and FINN fire emissions (Fig. 11). It generates global chemical initial and boundary conditions for regional-scale modeling, supported by meteorological inputs from the IITM-IMD GFS forecast at 12.5 km resolution. The regional setup operates at 10 km resolution, incorporating HTAP-V2 emissions, FINN fire emissions, biogenic sources and dynamic inputs from satellite data (*e.g*., AOD, NO_2, CO). Chemical data assimilation improves initialization accuracy through the Grid point Statistical Interpolation (GSI) system, which assimilates MODIS Aerosol Optical Depth (AOD) data from Terra and Aqua satellites at 06 UTC and 09 UTC, respectively. A background error covariance matrix is generated, accounting for 100% uncertainty in both anthropogenic and biomass burning emission sources, as supported by literature. A custom preprocessor for MODIS Collection 6.1 observations was also developed to enhance data processing efficiency. More details of the WRF-Chem and its skill can be found in Ghude *et al* (2020), Govardhan *et al* (2023), Jena *et al* (2021) and Kalita *et al*., 2023)

At the city scale, the setup focuses on high-resolution (400 m x 400 m) emission inventories for Delhi and surrounding regions, incorporating real-time emission processors and near-real-time fire emission predictions for up to three days. This setup leverages tagged tracers for source apportionment and scenario forecasting, enabling fine-grained air quality forecasts for air quality, extreme events, dust and haze. Together, the system demonstrates a robust capability to model air quality dynamics across scales, improving the understanding of pollution sources and enabling targeted interventions. This comprehensive framework is crucial for addressing air quality challenges in urban environments, particularly in regions like Delhi that face significant pollution-related risks.

6.2. *FMI-IMD-SILAM*

The System for Integrated Modeling of Atmospheric Composition (SILAM) offline 3-D chemistry transport model (Sofiev *et al*., 2015) is coupled with IMD-WRF meteorological model to predict surface particulate matter ($PM_{2.5}$ and PM_{10}) and gaseous pollutant concentrations over the Indian region with horizontal grid spacing of 3 km x 3 km. The current operational version is based on a Lagrangian dispersion model that applies an iterative advection algorithm and a Monte Carlo random-walk diffusion representation. The schematic diagram of IMD-SILAM model is shown in Fig. 12. The model has been widely used to simulate the air quality in regional and global scale (Brasseur *et al*., 2019; Kouznetsov *et al*., 2020). For the initial and boundary conditions (ICs/BCs) of meteorology are obtained from IMD-WRF Regional Forecasting System at 3 km resolution every hour. The chemical boundary conditions are obtained from the SILAM global forecasting system every three hours. The model uses CBM5 gas-phase chemistry supplemented with secondary organics, DMAT_SULPHUR Sulphur oxidation and simple equilibrium scheme for secondary inorganic aerosols, Volatile Basis-Set (VBS) for secondary organics of aerosol processor. The anthropogenic emissions of aerosols and trace gases (OC, BC, CO, NOx, *etc*.) are based on the CAMS-GLOB v2.1 0.1-deg supplemented with EDGAR v4.3.2 for coarse and mineral-fine particles for the year 2019 at 0.1º x 0.1º grid resolution. The dust and sea salt emissions are calculated online SILAM dust and sea

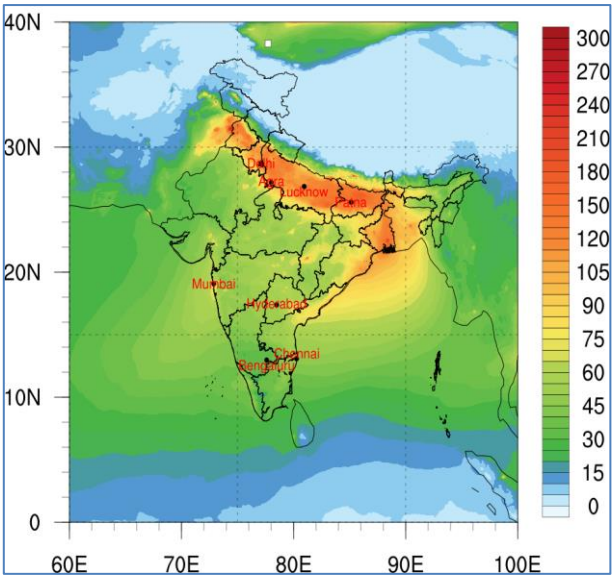

Fig. 13. Spatial distribution of average PM2.5 (µg/m^3) concentrations at 3 km horizontal grid-spacing of SILAM model (from day 1 forecast) over India during Dec 02, 2020 to Feb 28, 2021

salt scheme respectively. Emissions from biogenic are calculated online using the Model of Emissions of Gases and Aerosols from Nature version 2.1 (MEGAN2.1) (Guenther *et al*., 2006). The simulations are reinitialized from the chemistry fields of previous day of simulation.

Performance verification of the operational SILAM Model showed good skill over Indian region. Fig. 13 shows the spatial distribution of averaged $PM_{2.5}$ concentrations from SILAM model day-1 forecast (3 km grid spacing) for the period December 2, 2020 to February 28, 2021. It highlights elevated $PM_{2.5}$ concentrations over the Indo-Gangetic Plain (IGP) during winter season. This pollution hotspot region is characterized by high population density, frequent stagnant winds, temperature inversions and shallow boundary-layer heights during winter, fosters pollutant accumulation. Fig.14 presents the comparison of observed hourly mean values of $PM_{2.5}$ with SILAM model $PM_{2.5}$ values. The analysis reveals that SILAM model effectively captures $PM_{2.5}$ variability, including diurnal and synoptic-scale patterns. The model also successfully captures the sudden rise and fall in $PM_{2.5}$ concentration values due to meteorological factors such as variation in wind speed and direction, rainfall *etc*. However, it overestimates $PM_{2.5}$, particularly in January during low-concentration episodes. Ongoing efforts aim to address uncertainties in meteorological data, emissions, and chemical processes to improve model accuracy.

The skill scores (false alarm rate (FAR), probability of detection (POD) or hit rate, critical success index (CIS), bias and accuracy) for AQI categories (Unhealthy: AQI > 201, PM2.5 > 91 µg/m³; Very Unhealthy: AQI > 301, PM2.5 > 121 µg/m³) have been determined. The skill scores for Unhealthy pollution episodesindicate that the forecast accuracy exceeds 75% across India and IGP cities (Delhi, Agra, Lucknow, Patna). False alarm rates (FAR) are below 15%, while the probability of detection (POD) exceeds 80%, indicating reliable performance. For Very Unhealthy Events, while the POD remains high (>78%), the critical success index (CSI) is moderately lower (~0.65–0.71), and FAR increases (~11–33%).

For Delhi/NCR, the Unhealthy category accuracy exceeds 83%, with FAR ~5% and strong POD and CSI (~0.8). Very Unhealthy forecasts show higher FAR (~11%) but maintain good accuracy. For Agra, the Unhealthy forecast accuracy exceeds 73%, with slightly lower CSI (~0.68) and higher FAR (~13%). For Lucknow and Patna, the forecasts exhibit over 80% accuracy for Unhealthy Events and consistent performance for Very Unhealthy Events, with FAR ranging from ~12% to ~33%.

6.3. *High resolution street level air quality forecast model environmental information fusion service (ENFUSER)*

ENFUSER (The Finnish Meteorological Institute's ENvironmental information FUsion SERvice), is an operational, adaptive local-scale dispersion model. Technically, the model is a combination of Gaussian Puff and Gaussian Plume-style of dispersion modelling that utilizes measurement data to perform data fusion. The long-range transportation of pollutants are handled in the model by nesting the local-scale modelling on a regional-scale mode's concentration fields The aim of the data fusion is to adapt the dispersion modelling on an hourly basis to gain higher level of agreement with measurements; technically this is done by modifying emission factors for known sources and adjusting background concentrations, while simultaneously benchmarking measurement reliability. Further, on a longer term analysis period more realistic parametrization for emission sources can be obtained via the data fusion process, which after a while begins to show distinguishable trends and patterns for emission factors.

In addition to traditional dispersion model input, the model uses and assimilates a large amount of Geographic Information System data (GIS) to describe the modelling area on a high resolution such as a detailed description of the road network, buildings, land-use information, high-resolution satellite images, ground elevation and population data. The details of ENFUSER can be found in Johansson *et al*. (2022) and references there in.

The overall configuration of FMI-IMD ENFUSER for Delhi is illustrated in the Figure 15. The details of set up are presented in Table 8.

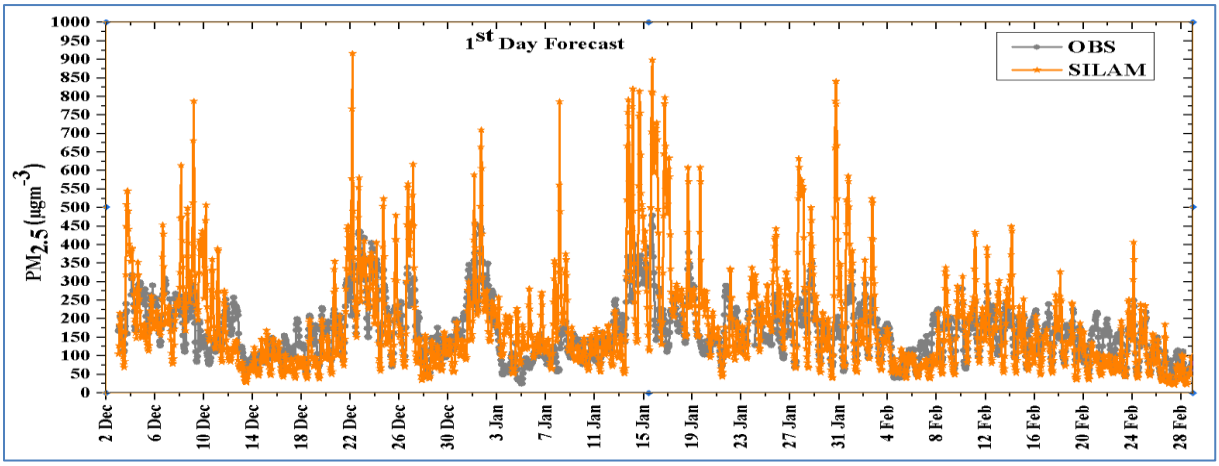

Fig.14. Comparison between hourly mean PM2.5 forecast (orange) and hourly mean PM2.5 averaged over 39 air quality monitoring stations (grey) on day one forecast over Delhi during 03 Dec 2020 to 28 Feb 2021

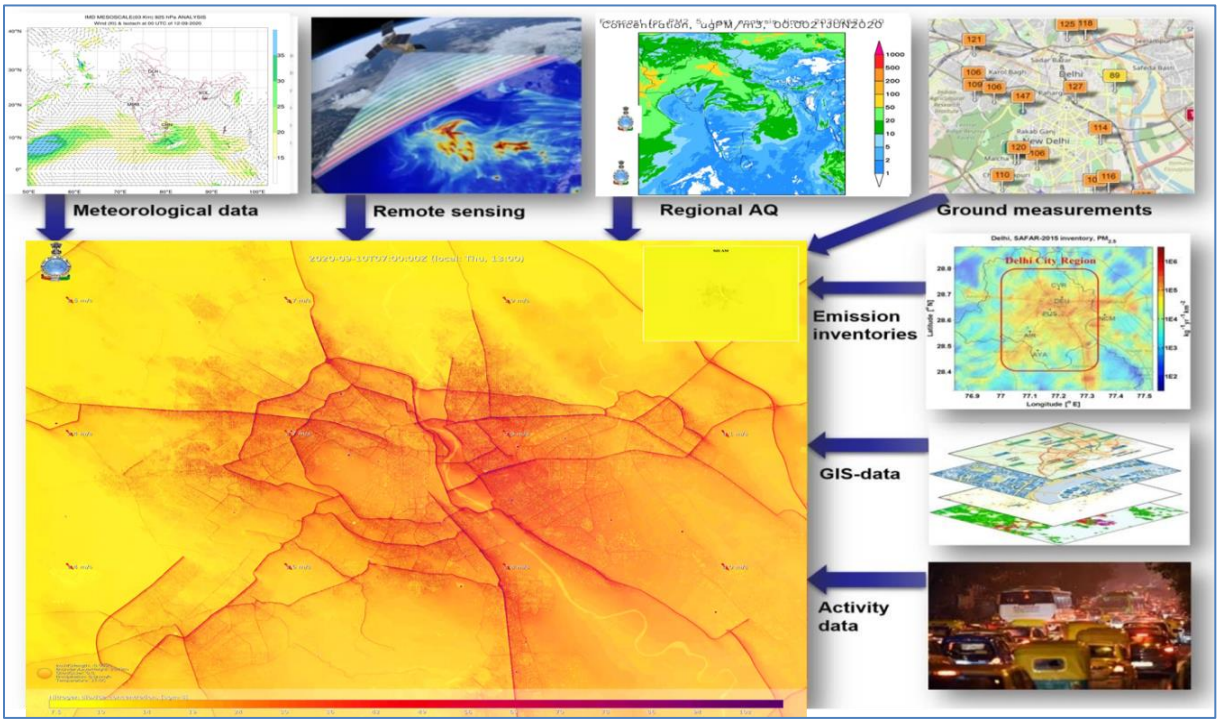

Fig. 15: The ENFUSER modelling conceptual framework

TABLE 8

ENFUSER set up details for New Delhi

Parameter	Details
Domain range, Latitude	28.362N - 28.86N
Domain range, Longitude	76.901E - 77.56E
Spatial resolution	27m (inner areas with higher resolution can be added)
Temporal resolution	1h averages
Modelled species	NO_2, $PM_{2.5}$, PM_{10}, O_3, coarse PM, SO_2, CO
Modelling time span	>48h per model run, updated several times a day
Main output formats	netCDF, statistics as CSV
Secondary output formats	animations (avi), GIF, Figures (PNG)
Output storage	Local (compressed) and optionally AWS S3 cloud storing

7. Conclusions and future directions

Environmental meteorology is critical to the protection of the environmental air quality and human health. As the human population continues to grow, the industrial development and energy use also continues to expand. Consequently, pollution remains inevitable and despite of significant advances in pollution control efforts. IMD has a long legacy of monitoring climate and air quality and environmental parameters such as precipitation chemistry, solar radiation, atmospheric ozone, carbonaceous and non-carbonaceous aerosol optical and physical properties and atmospheric chemistry. This review underscores the advancements India has made in addressing environment meteorology through technological innovations, advanced forecasting systems, and community engagement.

The air quality early warning system represents one of the most far-reaching development and practical applications of environment meteorology and numerical prediction, poses unprecedented scientific, technical, and computational challenges, and generates significant opportunities for science dissemination and community participations. The air quality forecast model SILAM showcases robust capabilities in forecasting unhealthy air quality events, particularly within the IGP region. Although predictions for very unhealthy events require further improvement, ongoing refinements are expected to enhance accuracy and reliability in extreme pollution episode forecasting. Challenges include simulating boundary-layer dynamics, synoptic advection, and aerosol processes, which can hinder predictions of extreme pollution events. Future studies will focus on refining these aspects for enhanced model performance.

IMD's historical contributions have not only improved the scientific understanding of atmospheric environment but also played a critical role in global efforts to combat air pollution and climate change. The information generated from long-term systematic measurements from environment monitoring network significantly contributed towards evidence based policy decisions, on international treaties like the Montreal Protocol and the Paris Agreement. Through sustained efforts in atmospheric monitoring and research, IMD continues to be a cornerstone in India's environmental and climatic resilience.

The continuous air quality monitoring systems are often expensive and limited in coverage. Innovations in low-cost, portable sensors are addressing this gap by providing cost-effective solutions for widespread monitoring. However, low-cost sensors are extremely new, and much research remains to be done to integrate these technologies. Special emphasis should be given to the quality check of the sensor's performance against conventional methods. Rural regions in India remain under-observed related to meteorological and air quality monitoring, despite being significantly affected by biomass burning and natural dust. Enhancing data collection from these areas is essential for achieving a comprehensive understanding of regional air quality.

The meteorology has a strong impact on air quality, and in return atmospheric composition has potentially strong feedback to weather and climate. There is a strong need to integrate atmospheric composition, weather and climate research to achieve a comprehensive description and understanding of the Earth System (WMO, 2016).

Emission inventories are the key input to the air quality modelling system, and many studies point to emission inventories as the most uncertain factor among the different components of air quality models. This uncertainty can be especially large for some activity sectors such as agriculture waste burning, fire crackers etc due to the lack of knowledge on the activities producing emissions. Most Representative emission inventories at the street level are hence crucial to air quality early warning system. A high-resolution dynamic emission inventory of air pollutants with near real time update of sources will be improve the accuracy of air quality forecast and effective mitigation measures.

Acknowledgement

The authors express their sincere gratitude to the Director General of Meteorology for their invaluable support. Special thanks are also extended to all past and present officers who have led Environment Monitoring Research Centre (EMRC). The authors acknowledge the contributions of numerous scientists from IMD, IITM and NCMRWF whose work, though not directly cited, has significantly advanced the quality of environmental monitoring and air quality early warning services dedicated to the nations.

Disclaimer: The contents and views presented in this research article/paper are the views of the authors and do not necessarily reflect the views of the organizations they belongs to.

References

Abish, B., Mohanakumar, K., 2011, "Role of fine mode aerosols in modulating cloud properties over industrial locations in north India", *Ann. Geophys.* **29**, 1605-1612. doi : https://doi.org/10.5194/angeo-29-1605-2011.

Ali, K., Trivedi, D. K., Sahu, S. K., 2017, "Surface ozone characterization at Larsemann Hills and Maitri, Antarctica", *Science of The Total*

Environment 584-585, 1130-1137. doi : https://doi.org/10.1016/j.scitotenv.2017.01.173.

Anderson, D. E., Cahalan, R. F., 2005, "The solar radiation and climate experiment (SORCE) mission for the NASA earth observing system (eos)", *Solar Physics*, **230**, 3-6.

Anil Kumar, V., Pandithurai, G., Leena, P. P., Dani, K. K., Murugavel, P., Sonbawne, S. M., Patil, R. D. and Maheskumar, R. S., 2016, "Investigation of aerosol indirect effects on monsoon clouds using ground-based measurements over a high-altitude site in Western Ghats", *Atmospheric Chemistry and Physics*, **16**, 8423-8430.

Ansari, K., Pandithurai, G., Kumar, V.A., 2020, "Role of droplet size classes on the cloud droplet spectral dispersion as observed over the Western Ghats", *Atmospheric research*, **246**, 105104.

Babu, S. S., Satheesh, S. K., Moorthy, K. K., 2002, "Aerosol radiative forcing due to enhanced black carbon at an urban site in India, "*Geophysical Research Letters* **29**", doi : https://doi.org/10.1029/2002GL015826.

Beig, G., Chate, D. M., Ghude, S. D., Ali, K., Satpute, T., Sahu, S. K., Parkhi, N., Trimbake, H. K., 2013, "Evaluating population exposure to environmental pollutants during Deepavali fireworks displays using air quality measurements of the SAFAR network", *Chemosphere* **92**, 116-124. doi : https://doi.org/10.1016/j.chemosphere.2013.02.043.

Beig, G., Chate, D. M., Sahu, S. K., Parkhi, N. S., Srinivas, R., Ali, K., Ghude, S. D., Yadav, S., Trimbake, H. K., 2015, "System of air quality forecasting and research (SAFAR-India)", World Meteorological Organization Global Atmosphere Watch, Report.

Beig, G., Sahu, S. K., Anand, V., Bano, S., Maji, S., Rathod, A., Korhale, N., Sobhana, S.B., Parkhi, N., Mangaraj, P., Srinivas, R., Peshin, S.K., Singh, S., Shinde, R., Trimbake, H.K., 2021, "India's Maiden air quality forecasting framework for megacities of divergent environments: The SAFAR-project" *Environmental Modelling & Software* **145**, 105204. https://doi.org/10.1016/j.envsoft.2021.105204.

Bhaskar, V. V., Safai, P., Raju, M., 2015, "Long term characterization of aerosol optical properties: Implications for radiative forcing over the desert region of Jodhpur, India", *Atmospheric Environment* **114**, 66-74.

Bhaskar, V. V., Soni, V., Panicker, A., 2017, "Long term characteristics of aerosols over Pune, central India-Effect on radiative forcing", *Mausam* **68**, 119-130.

Bhattacharya, B. K., Nigam, R., 2015, "INSAT-3D product algorithm theoretical basis document", ATBD Document, 335-360.

Bond, T. C., Bergstrom, R. W., 2006, "Light Absorption by Carbonaceous Particles: An Investigative Review", *Aerosol Science and Technology* **40**, 27-67. doi : https://doi.org/10.1080/02786820500421521.

Bond, T. C., Doherty, S. J., Fahey, D. W., Forster, P. M., Berntsen, T., DeAngelo, B. J., Flanner, M. G., Ghan, S., Kärcher, B., Koch, D., Kinne, S., Kondo, Y., Quinn, P. K., Sarofim, M. C., Schultz, M. G., Schulz, M., Venkataraman, C., Zhang, H., Zhang, S., Bellouin, N., Guttikunda, S. K., Hopke, P. K., Jacobson, M. Z., Kaiser, J. W., Klimont, Z., Lohmann, U., Schwarz, J. P., Shindell, D., Storelvmo, T., Warren, S. G., Zender, C. S., 2013, "Bounding the role of black carbon in the climate system: A scientific assessment: BLACK CARBON IN THE CLIMATE SYSTEM", *J. Geophys. Res. Atmos*. **118**, 5380–5552. https://doi.org/10.1002/jgrd.50171.

Brasseur, G. P., Xie, Y., Petersen, A. K., Bouarar, I., Flemming, J., Gauss, M., Jiang, F., Kouznetsov, R., Kranenburg, R., Mijling, B., Peuch, V.-H., Pommier, M., Segers, A., Sofiev, M., Timmermans, R., Van Der A, R., Walters, S., Xu, J., Zhou, G., 2019, "Ensemble forecasts of air quality in eastern China – Part 1: Model description and implementation of the MarcoPolo–Panda prediction system, version 1", *Geosci. Model Dev*. **12**, 33–67. https://doi.org/10.5194/gmd-12-33-2019.

Bright, J. M., 2019, "Solcast: Validation of a satellite-derived solar irradiance dataset", *Solar Energy* **189**, 435–449. https://doi.org/10.1016/j.solener.2019.07.086.

Chacko, O. and Desikan, V., 1965, "Atmospheric turbidity measurements over India", *MAUSAM* **16**, 649–660. https://doi.org/10.54302/mausam.v16i4.5695.

Chamberlain-Ward, S. and Sharp, F., 2011, "Advances in Nephelometry through the Ecotech Aurora Nephelometer", *The Scientific World JOURNAL* **11**, 2530-2535. https://doi.org/10.1100/2011/310769.

Charlson, R. J., Ahlquist, N. C., Selvidge, H. and MacCready, P. B., 1969, "Monitoring of Atmospheric Aerosol Parameters with the Integrating Nephelometer", *Journal of the Air Pollution Control Association* **19**, 937–942. https://doi.org/10.1080/00022470.1969.10469360.

Charlson, R. J., Langner, J., Rodhe, H., Leovy, C. B. and Warren, S.G., 1991, "Perturbation of the northern hemisphere radiative balance by backscattering from anthropogenic sulfate aerosols", *Tellus A: Dynamic Meteorology and Oceanography* **43**, 152. https://doi.org/10.3402/tellusa.v43i4.11944.

Charlson, R. J., Schwartz, S. E., Hales, J. M., Cess, R. D., Coakley, J. A., Hansen, J. E. and Hofmann, D. J., 1992, "Climate Forcing by Anthropogenic Aerosols", *Science* **255**, 423-430. https://doi.org/10.1126/science.255.5043.423.

Chiplonkar, M. W., 1939, "Measurements of atmospheric ozone at Bombay", *Proc. Indian Acad. Sci. (Math.Sci.)* **10**, 105–120. https://doi.org/10.1007/BF03170429.

Das, D. K., Dev Burman, G. K., Kidwai, A. L., 1981, "Chemical composition of monsoon rainwater over Bhopal) Madhya Pradesh (India) during 1977 and 1978, "*MAUSAM* , **32**, 221–228. https://doi.org/10.54302/mausam.v32i3.3369.

Desikan, V., Chivate, V. R., Abhyankar, V. V., 1994a, "Reaction of radiometric parameters to atmospheric pollution : part ii -a comparative study between pairs of stations", *MAUSAM*, **45**, 139–148. https://doi.org/10.54302/mausam.v45i2.2072.

Desikan, V., Chivate, V. R., Abihyankar, V. V., 1994b, "Reaction of radiometric parameters to atmospheric pollution: Part I - Variation over time" *MAUSAM*, **45**, 79–86. https://doi.org/10.54302/mausam.v45i1.1888.

Desikan, V., Iyer, N. and Rahalkar, C., 1969, "Diffuse solar (sky) radiation measurements over India}, *MAUSAM* **20**, 389–394. https://doi.org/10.54302/mausam.v20i4.5777.

Devara, P. C. S., Jadhav, D. R. and Ernest Raj, P., 1986, "Some Design Aspects of Lidar System for Measurement of Atmospheric Aersosols", *J Opt* **15**, 21–25. https://doi.org/10.1007/BF03549143.

Dey, S., Tripathi, S., 2007.Estimation of aerosol optical properties and radiative effects in the Ganga basin, northern India, during the wintertime. Journal of Geophysical Research: Atmospheres 112.

Dipu, S., Prabha, T. V., Pandithurai, G., Dudhia, J., Pfister, G., Rajesh, K., Goswami, B. N., 2013, "Impact of elevated aerosol layer on the cloud macrophysical properties prior to monsoon onset",

Atmospheric Environment **70**, 454–467. https://doi.org/10.1016/j.atmosenv.2012.12.036.

Dobson, G. M. B., Harrison, D. M., 1926, "Measurements of the amount of ozone in the earth's atmosphere and its relation to other geophysical conditions", *Proc. R. Soc. Lond*. A **110**, 660–693. https://doi.org/10.1098/rspa.1926.0040.

Dobson, G. M. B., Kimball, H. H., Kidson, E., 1930, "Observations of the Amount of Ozone in the Earth's Atmosphere, and Its Relation to Other Geophysical Conditions", Part IV. Proceedings of the Royal Society of London. Series A, Containing Papers of a Mathematical and Physical Character **129**, 411–433.

Drinovec, L., Močnik, G., Zotter, P., Prévôt, A. S. H., Ruckstuhl, C., Coz, E., Rupakheti, M., Sciare, J., Müller, T., Wiedensohler, A., Hansen, A. D. A., 2015, "The "dual-spot" Aethalometer: an improved measurement of aerosol black carbon with real-time loading compensation", *Atmos. Meas. Tech*. **8**, 1965–1979. https://doi.org/10.5194/amt-8-1965-2015.

Fabry, Ch. and Buisson, H., 1913, "L'absorption de l'ultra-violet par l'ozone et la limite du spectre solaire", *J. Phys. Theor. Appl*. **3**, 196–206. https://doi.org/10.1051/jphystap:019130030019601.

Féry, C., 1911, "A prism with curved faces, for spectrograph or spectroscope", *Astrophysical Journal*, **34**, p. 79, 34, 79.

Ganguly, N. D., 2013, "High surface ozone episodes at Maitri in Antarctica, "*Indian J Phys*, **87**, 947–951. https://doi.org/10.1007/s12648-013-0325-1.

Ghude, S. D., Kumar, R., Jena, C., Debnath, S., Kulkarni, R. G., Alessandrini, S., Biswas, M., Kulkrani, S., Pithani, P., Kelkar, S., Sajjan, V., Chate, D. M., Soni, V. K., Singh, S., Nanjundiah, R. S. and Rajeevan, M., 2020, "Evaluation of PM2.5 forecast using chemical data assimilation in the WRF-Chem model", *Current Science*, **118**, 1803-1815.

Götz, F. P., Meetham, A., Dobson, G. M. B., 1934, "The vertical distribution of ozone in the atmosphere, "Proceedings of the Royal Society of London", Series A, Containing Papers of a Mathematical and Physical Character **145**, 416-446.

Götz, F. W. P., 1931, "Zum Strahlungsklima des Spitzbergensommers: Strahlungs-und Ozonmessungen in der Königsbucht 1929.

Govardhan, G., Ambulkar, R., Kulkarni, S., Vishnoi, A., Yadav, P., Choudhury, B. A., Khare, M., Ghude, S. D., 2023, "Stubble-burning activities in north-western India in 2021: Contribution to air pollution in Delhi. *Heliyon* **9**, e16939. https://doi.org/10.1016/j.heliyon.2023.e16939.

Guenther, A., Karl, T., Harley, P., Wiedinmyer, C., Palmer, P. I., Geron, C., 2006, "Estimates of global terrestrial isoprene emissions using MEGAN (Model of Emissions of Gases and Aerosols from Nature)", *Atmos. Chem. Phys*. **6**, 3181-3210. https://doi.org/10.5194/acp-6-3181-2006.

Handa, B., 1968, "Chemical composition of rain water in some parts of northern India-Preliminary studies", *MAUSAM* **19**, 175–180. https://doi.org/10.54302/mausam.v19i2.5233.

Handa, B., 1969. Chemical Compostion Of Rain Water Over Calcutta. *MAUSAM* **20**, 150-154. https://doi.org/10.54302/mausam.v20i2.5446

Handa, B. K., 1971, "Chemical Composition of Monsoon Rainwater Over Bankipur, Malda (West Bengal), *MAUSAM* **22**, 603–604. https://doi.org/10.54302/mausam.v22i4.5026.

Handa, B. K., Kumar, A. and Goel, D.K., 1982, "Chemical composition of rain water over Lucknow in 1980", *MAUSAM* **33**, 485–488. https://doi.org/10.54302/mausam.v33i4.2611.

Harikishan, G., Padmakumari, B., Maheskumar, R., Pandithurai, G., Min, Q., 2016, "Aerosol indirect effects from ground-based retrievals over the rain shadow region in Indian subcontinent" *Journal of Geophysical Research: Atmospheres* **121**, 2369–2382.

Heintzenberg, J. and Charlson, R. J., 1996, "Design and Applications of the Integrating Nephelometer: A Review", *J. Atmos. Oceanic Technol*. 13, 987–1000. https://doi.org/10.1175/1520-0426(1996)013<0987:DAAOTI>2.0.CO;2

Hess, M., Koepke, P., Schult, I., 1998, "Optical properties of aerosols and clouds: The software package OPAC", *Bulletin of the American meteorological society* **79**, 831–844.

Jacobson, M. Z., 2001, "Strong radiative heating due to the mixing state of black carbon in atmospheric aerosols" *Nature* **409**, 695–697. https://doi.org/10.1038/35055518.

Jayaraman, A., Lubin, D., Ramachandran, S., Ramanathan, V., Woodbridge, E., Collins, W.D., Zalpuri, K.S., 1998, "Direct observations of aerosol radiative forcing over the tropical Indian Ocean during the January-February 1996 pre-INDOEX cruise", *J. Geophys. Res*. **103**, 13827–13836. https://doi.org/10.1029/98JD00559.

Jena, C., Ghude, S. D., Kumar, R., Debnath, S., Govardhan, G., Soni, V. K., Kulkarni, S. H., Beig, G., Nanjundiah, R. S., Rajeevan, M., 2021, "Performance of high resolution (400 m) PM2.5 forecast over Delhi", *Sci Rep* **11**, 4104. https://doi.org/10.1038/s41598-021-83467-8.

Johansson, L., Karppinen, A., Kurppa, M., Kousa, A., Niemi, J. V., and Kukkonen, J., 2022, "An operational urban air quality model ENFUSER, based on dispersion modelling and data assimilation", *Environmental Modelling & Software*, **156**, 105460. https://doi.org/10.1016/j.envsoft.2022.105460.

Kalita, G., Yadav, P. P., Jat, R., Govardhan, G., Ambulkar, R., Kumar, R., Gunwani, P., Debnath, S., Sharma, P., Kulkarni, S., Kaginalkar, A. and Ghude, S. D., 2023, "Forecasting of an unusual dust event over western India by the Air Quality Early Warning System", *Atmospheric Environment* **311**, 120013. https://doi.org/10.1016/j.atmosenv.2023.120013.

Kanawade, V. P., Srivastava, A. K., Ram, K., Asmi, E., Vakkari, V., Soni, V. K., Varaprasad, V., Sarangi, C., 2020, "What caused severe air pollution episode of November 2016 in New Delhi?", *Atmospheric Environment* **222**, 117125. https://doi.org/10.1016/j.atmosenv.2019.117125.

Karandikar, R., 1948, "Studies in atmospheric ozone", *Proceedings Mathematical Sciences*, **28**, 63–85.

Kaufman, Y. J., Tanré, D., Boucher, O., 2002, "A satellite view of aerosols in the climate system", *Nature* **419**, 215–223. https://doi.org/10.1038/nature01091.

Kouznetsov, R., Sofiev, M., Vira, J., Stiller, G., 2020, "Simulating age of air and the distribution of SF₆ in the stratosphere with the SILAM model", *Atmos. Chem. Phys*. **20**, 5837–5859. https://doi.org/10.5194/acp-20-5837-2020.

Kren, A. C., Pilewskie, P., Coddington, O., 2017, "Where does Earth's atmosphere get its energy?" *J. Space Weather Space Clim*. **7**, A10. https://doi.org/10.1051/swsc/2017007.

Kulkarni, J. R., Maheskumar, R. S., Morwal, S. B., Kumari, B. P., Konwar, M., Deshpande, C. G., Joshi, R. R., Bhalwankar, R. V., Pandithurai, G., Safai, P. D., Narkhedkar, S. G., Dani, K. K., Nath, A., Nair, S., Sapre, V. V., Puranik, P. V., Kandalgaonkar, S. S., Mujumdar, V. R., Khaladkar, R. M., Vijayakumar, R., Prabha, T. V., Goswami, B. N., 2012, "The Cloud Aerosol

Interaction and Precipitation Enhancement Experiment (CAIPEEX): overview and preliminary results", *Current Science* **102**, 413–425.

Kulkarni, S. H., Ghude, S. D., Jena, C., Karumuri, R. K., Sinha, B., Sinha, V., Kumar, R., Soni, V. K. and Khare, M., 2020, "How Much Does Large-Scale Crop Residue Burning Affect the Air Quality in Delhi?", *Environ. Sci. Technol*. **54**, 4790–4799. https://doi.org/10.1021/acs.est.0c00329.

Kumar, R. R., 2020, Evaluation of spatial and temporal heterogeneity of black carbon aerosol mass concentration over India using three year measurements from IMD BC observation network. Science of the Total Environment 12.

Kumar, V., Bist, S., Akram, R., Kumar, A., Soni, V.K., Chug, S., 2023a. "Evaluation of meteorological characteristics and the influence of the Southern Annular Mode at newly established Bharati Station, East Antarctica" *Polar Science* 101010. https://doi.org/10.1016/j.polar.2023.101010.

Kumar, V., Devara, P. C. S., Soni, V. K., 2023b, Multisite Scenarios of Black Carbon and Biomass Burning Aerosol Characteristics in India. *Aerosol Air Qual. Res*. **23**, 220435. https://doi.org/10.4209/aaqr.220435.

Lal, R. P., Ram, S., 2013, "Compilation of ozonesonde observation over Schirmacher oasis east Antarctic from 1999-2007", *MAUSAM* **64**, 613–624. https://doi.org/10.54302/mausam.v64i4.744.

Loeb, N. G., Kato, S., Su, W., Wong, T., Rose, F.G., Doelling, D. R., Norris, J. R. and Huang, X., 2012, "Advances in understanding top-of-atmosphere radiation variability from satellite observations", *Surveys in geophysics* **33**, 359–385.

Mani, A., 1971, "Radiation balance of the earth-atmosphere systems from satellite radiation measurements", *MAUSAM* **22**, 455–460. https://doi.org/10.54302/mausam.v22i3.4945.

Mani, A., 1981, Handbook of solar radiation data for India, 1980.

Mani, A., Chacko, O., 1963a, "Studies of Nocturnal Radiation at Poona and Delhi", *MAUSAM* **14**, 196–204. https://doi.org/10.54302/mausam.v14i2.203.

Mani, A., Chacko, O., 1963b, "Measurements of Diffuse Solar Radiation at Delhi and Poona", *MAUSAM* **14**, 416–432. https://doi.org/10.54302/mausam.v14i4.5491.

Mani, A., Chacko, O. and Desikan, V., 1977, "Solar radiation measurements and studies of atmospheric transmission at high altitude stations in India", *MAUSAM* **28**, 51–62. https://doi.org/10.54302/mausam.v28i1.2664.

Mani, A., Chacko, O., Desikan, V., Krishnamurthy, V., 1967, "Distribution of global and net solar radiation over the Indian Ocean", *MAUSAM* **18**, 171–184. https://doi.org/10.54302/mausam.v18i2.4428.

Mani, A., Chacko, O., Venkiteshwaran, S. P., 1962a, "Measurements of the total Radiation from Sun and Sky in India during the IGY", *MAUSAM* **13**, 337–366. https://doi.org/10.54302/mausam.v13i3.4367.

Mani, A., Rangarajan, S., 1982, "Solar radiation over India", Allied Publishers.

Mani, A., Swaminathan, M. S., Venkiteshwaran, S. P., 1962b, "Distribution of sunshine and solar radiation over the Indian Peninsula", *MAUSAM* **13**, 195–212. https://doi.org/10.54302/mausam.v13i2.4338.

Manoj, M., Devara, P., Joseph, S., Sahai, A., 2012, "Aerosol indirect effect during the aberrant Indian Summer Monsoon breaks of 2009", *Atmospheric Environment* **60**, 153–163.

Maske, S. J., Nand, K., 1982, "Studies on chemical constituents of precipitation over India" *MAUSAM* **33**, 241–246. https://doi.org/10.54302/mausam.v33i2.3169.

Mooley, D. A. and Raghavan, S., 1963, "Total radiation from Sun and Sky on a horizontal surface in relation to cloud type at Madras", *MAUSAM* **14**, 483–485. https://doi.org/10.54302/mausam.v14i4.5501.

Mor, V., Dhankhar, R., Attri, S. D., Soni, V. K., Sateesh, M. and Taneja, K., 2017, "Assessment of aerosols optical properties and radiative forcing over an Urban site in North-Western India", *Environmental Technology* **38**, 1232–1244. https://doi.org/10.1080/09593330.2016.1221473.

Mukherjee, A., Nand, K., Mukhopadhyay, B., Ghanekar, S., 1986, "Rainwater chemistry over Indian sea areas during monsoon season" *MAUSAM* **37**, 173–178. https://doi.org/10.54302/mausam.v37i2.2222.

Mukherjee, A. K., 1956, "Salinity In Rain Water", *MAUSAM* **7**, 84–87. https://doi.org/10.54302/mausam.v7i1.4519.

Mukherjee, A. K., 1957, "H+ ion concentration of monsoon rainwater at Calcutta. *MAUSAM* **8**, 321–324. https://doi.org/10.54302/mausam.v8i3.5048.

Mukherjee, A. K., 1964, "Acidity of Monsoon Rain Water", *MAUSAM* **15**, 267–270. https://doi.org/10.54302/mausam.v15i2.5541.

Mukherjee, A. K., 1978, "pH of monsoon rain water over Bay of Bengal", *MAUSAM* **29**, 749. https://doi.org/10.54302/mausam.v29i4.2959

Mukhopadhyay, B., Datar, S.V., Srivastava, H.N., 1992, "Precipitation chemistry over the Indian region", *MAUSAM* **43**, 249–258. https://doi.org/10.54302/mausam.v43i3.3450.

Mukhopadhyay, B., Singh, S.S., Datar, S.V., 1993, "Principal component analysis of rainwater composition at BAPMoN stations in India", *MAUSAM* **44**, 179–184. https://doi.org/10.54302/mausam.v44i2.3817.

Myhre, G., Shindell, D., Bréon, F.-M., Collins, W., Fuglestvedt, J., Huang, J., Koch, D., Lamarque, J.-F., Lee, D., Mendoza, B., Nakajima, T., Robock, A., Stephens, G., Zhang, H., Aamaas, B., Boucher, O., Dalsøren, S.B., Daniel, J.S., Forster, P., Granier, C., Haigh, J., Hodnebrog, Ø., Kaplan, J.O., Marston, G., Nielsen, C.J., O'Neill, B.C., Peters, G.P., Pongratz, J., Ramaswamy, V., Roth, R., Rotstayn, L., Smith, S.J., Stevenson, D., Vernier, J.-P., Wild, O., Young, P., Jacob, D., Ravishankara, A.R., Shine, K., 2013. 8 Anthropogenic and Natural Radiative Forcing. IPCC AR5, 82.

Nair, V. S., Babu, S. S., Manoj, M., Moorthy, K. K., Chin, M., 2017, "Direct radiative effects of aerosols over South Asia from observations and modeling", *Climate Dynamics* **49**, 1411–1428.

Nakajima, T., Campanelli, M., Che, H., Estellés, V., Irie, H., Kim, S.-W., Kim, J., Liu, D., Nishizawa, T., Pandithurai, G., Soni, V.K., Thana, B., Tugjsurn, N.-U., Aoki, K., Go, S., Hashimoto, M., Higurashi, A., Kazadzis, S., Khatri, P., Kouremeti, N., Kudo, R., Marenco, F., Momoi, M., Ningombam, S.S., Ryder, C.L., Uchiyama, A., Yamazaki, A., 2020. An overview of and issues with sky radiometer technology and SKYNET. *Atmos. Meas. Tech*. **13**, 4195–4218. https://doi.org/10.5194/amt-13-4195-2020.

Nakajima, T., Yoon, S., Ramanathan, V., Shi, G., Takemura, T., Higurashi, A., Takamura, T., Aoki, K., Sohn, B., Kim, S., Tsuruta, H., Sugimoto, N., Shimizu, A., Tanimoto, H., Sawa, Y., Lin, N., Lee, C., Goto, D., Schutgens, N., 2007, "Overview of the Atmospheric Brown Cloud East Asian Regional Experiment

2005 and a study of the aerosol direct radiative forcing in east *Asia. J. Geophys. Res*. **112**, 2007JD009009. https://doi.org/10.1029/2007JD009009

Nand, K., 1984, "Prospects of acid rain over India", *MAUSAM* **35**, 225–232. https://doi.org/10.54302/mausam.v35i2.2017.

Nand, K., 1986, "Importance of natural dust in controlling the acidity of rain over India", *MAUSAM* **37**, 397–400. https://doi.org/10.54302/mausam.v37i3.2469

Nand, K., Maske, S.J., 1983. Atmospheric turbidity measurements with Volz sunphotometer at a few background air pollution monitoring network stations in India. MAUSAM 34, 327–330. https://doi.org/10.54302/mausam.v34i3.2489

Padma Kumari, B., Londhe, A.L., Daniel, S., Jadhav, D.B., 2007. Observational evidence of solar dimming: Offsetting surface warming over India. Geophysical Research Letters 34, 2007GL031133. https://doi.org/10.1029/2007GL031133

Padmakumari, B., Maheskumar, R.S., Anand, V., Axisa, D., 2017a. Microphysical characteristics of convective clouds over ocean and land from aircraft observations. Atmospheric Research 195, 62–71. https://doi.org/10.1016/j.atmosres.2017.05.011

Padmakumari, B., Soni, V.K., Rajeevan, M.N., 2017b. Trends in Radiative Fluxes Over the Indian Region, in: Rajeevan, M.N., Nayak, S. (Eds.), Observed Climate Variability and Change over the Indian Region, Springer Geology. Springer Singapore, Singapore, pp. 145–163. https://doi.org/10.1007/978-981-10-2531-0_9

Pandithurai, G., Dipu, S., Dani, K.K., Tiwari, S., Bisht, D.S., Devara, P.C.S., Pinker, R.T., 2008. Aerosol radiative forcing during dust events over New Delhi, India. J. Geophys. Res. 113, 2008JD009804. https://doi.org/10.1029/2008JD009804

Pandithurai, G., Dipu, S., Prabha, T.V., Maheskumar, R.S., Kulkarni, J.R., Goswami, B.N., 2012.Aerosol effect on droplet spectral dispersion in warm continental cumuli. J. Geophys. Res. 117, 2011JD016532. https://doi.org/10.1029/2011JD016532

Pandithurai, G., Pinker, R.T., Takamura, T., Devara, P.C.S., 2004. Aerosol radiative forcing over a tropical urban site in India.Geophysical Research Letters 31, 2004GL019702. https://doi.org/10.1029/2004GL019702

Panicker, A.S., Aditi, R., Beig, G., Ali, K., Solmon, F., 2018. Radiative Forcing of Carbonaceous Aerosols over Two Urban Environments in Northern India Abhilash S. Panicker , Rathod Aditi, Gufran Beig, Kaushar Ali, Fabien Solmon. Aerosol Air Qual. Res. 18, 884–894. https://doi.org/10.4209/aaqr.2017.01.0056

Panicker, A.S., Pandithurai, G., Dipu, S., 2010a. Aerosol indirect effect during successive contrasting monsoon seasons over Indian subcontinent using MODIS data. Atmospheric Environment 44, 1937–1943. https://doi.org/10.1016/j.atmosenv.2010.02.015

Panicker, A.S., Pandithurai, G., Safai, P.D., Dipu, S., Lee, D.-I., 2010b. On the contribution of black carbon to the composite aerosol radiative forcing over an urban environment. Atmospheric Environment 44, 3066–3070. https://doi.org/10.1016/j.atmosenv.2010.04.047

Panicker, A.S., Pandithurai, G., Safai, P.D., Kewat, S., 2008.Observations of enhanced aerosol longwave radiative forcing over an urban environment.Geophysical Research Letters 35, 2007GL032879. https://doi.org/10.1029/2007GL032879

Panicker, A.S., Pandithurai, G., Safai, P.D., Prabha, T.V., 2016.Indirect forcing of black carbon on clouds over northeast India.Quart J Royal Meteoro Soc 142, 2968–2973. https://doi.org/10.1002/qj.2878

Panicker, A.S., Sandeep, K., Negi, R.S., Gautam, A.S., Bisht, D.S., Beig, G., Murthy, B.S., Latha, R., Singh, S., Das, S., 2019. Estimates of Carbonaceous Aerosol Radiative Forcing over a Semiurban Environment in Garhwal Himalayas.Pure Appl. Geophys. 176, 5069–5078. https://doi.org/10.1007/s00024-019-02248-7

Pant, P. al, Hegde, P., Dumka, U., Sagar, R., Satheesh, S., Moorthy, K.K., Saha, A., Srivastava, M., 2006. Aerosol characteristics at a high-altitude location in central Himalayas: Optical properties and radiative forcing. Journal of geophysical research: Atmospheres 111.

Parameswaran, K., Rose, K.O., Murthy, B.V.K., 1984. Aerosol characteristics from bistatic lidar observations. J. Geophys. Res. 89, 2541–2552. https://doi.org/10.1029/JD089iD02p02541

Patel, P.N., Kumar, R., 2015. Estimation of aerosol characteristics and radiative forcing during dust events over Dehradun. Aerosol and Air Quality Research 15, 2082–2093.

Pathak, B., Kalita, G., Bhuyan, K., Bhuyan, P., Moorthy, K.K., 2010. Aerosol temporal characteristics and its impact on shortwave radiative forcing at a location in the northeast of India. Journal of Geophysical Research: Atmospheres 115.

Pathakoti, M., Asuri, L. K., Dangeti Venkata, M., Peethani, S., Gaddamidi, S., Soni, V. K., & Peshin, S. K. (2018). Assessment of total columnar ozone climatological trends over the Indian sub-continent. *International Journal of Remote Sensing*, *39*(12), 3963-3982. https://doi.org/10.1080/01431161.2018.1452066

Pathakoti, M., Santhoshi, T., Aarathi, M., Mahalakshmi, D., Kanchana, A., Srinivasulu, J., SS, R.S., Soni, V.K., MVR, S.S., Raja, P., 2021.Assessment of spatio-temporal climatological trends of ozone over the Indian region using machine learning.Spatial Statistics 43, 100513.

Peshin, S., Rao, P.R., Srivastav, S.K., 1997. Antarctic ozone depletion measured by balloonsondes at Maitri-1992. Mausam 48, 443–446.

Peshin, S.K., 2011. Study of SO2 and NO2 behaviour during the ozone-hole event at Antarctica by Brewer Spectrophotometer. MAUSAM 62, 595–600. https://doi.org/10.54302/mausam.v62i4.364

Peshin, S.K., Dewhare, J.N., Bhatia, R.C., Srivastav, S.K., 2000. Recent changes observed in column ozone concentrations over India. MAUSAM 51, 69–74. https://doi.org/10.54302/mausam.v51i1.1758

Peshin, S.K., Panda, N.C., Dewhare, J.N., Perov, S.P., 2003. Comparison of Indian ozonesonde and Umkehr profiles at New Delhi 1989-97. MAUSAM 54, 679–682. https://doi.org/10.54302/mausam.v54i3.1559

Petzold, A., Ogren, J.A., Fiebig, M., Laj, P., Li, S.-M., Baltensperger, U., Holzer-Popp, T., Kinne, S., Pappalardo, G., Sugimoto, N., Wehrli, C., Wiedensohler, A., Zhang, X.-Y., 2013. Recommendations for reporting "black carbon" measurements. Atmos. Chem. Phys. 13, 8365–8379. https://doi.org/10.5194/acp-13-8365-2013.

Prabha, T.V., Patade, S., Pandithurai, G., Khain, A., Axisa, D., Pradeep-Kumar, P., Maheshkumar, R.S., Kulkarni, J.R., Goswami, B.N., 2012. Spectral width of premonsoon and monsoon clouds over Indo-Gangetic valley. J. Geophys. Res. 117, 2011JD016837. https://doi.org/10.1029/2011JD016837.

Ramachandran, S., Kedia, S., 2010. Black carbon aerosols over an urban region: Radiative forcing and climate impact. J. Geophys. Res. 115, 2009JD013560. https://doi.org/10.1029/2009JD013560

Raman, P.K., 1938. Measurements of the radiation in the sky and the sky at Poona.Memoirs of India Meteorological Department 26.

Ramanathan, K., 1963. Bi-annual variation of atmospheric ozone over the tropics. Quarterly Journal of the Royal Meteorological Society 89, 540–542.

Ramanathan, K.R., 1961. Water vapour and ozone in the Atmosphere and stratospheric circulation. MAUSAM 12, 391–400. https://doi.org/10.54302/mausam.v12i3.4211

Ramanathan, K.R., Angreji, P.D., Shah, G.M., 1965. Ozone absorption coefficients and haze corrections for total ozone measurements with Dobson spectrophotometer. MAUSAM 16, 671–674. https://doi.org/10.54302/mausam.v16i4.5697

Ramanathan, V., Carmichael, G., 2008. Global and regional climate changes due to black carbon. Nature Geosci 1, 221–227. https://doi.org/10.1038/ngeo156

Ramanathan, V., Crutzen, P.J., Kiehl, J.T., Rosenfeld, D., 2001.Aerosols, Climate, and the Hydrological Cycle.Science 294, 2119–2124. https://doi.org/10.1126/science.1064034

Ramdas, L.A., Yegnanarayanan, S., 1956. Solar Energy in India.Proc. UNESCO Symp. Wind and Solar Energy, New Delhi 188–197.

Rangarajan, S., 1963.Seasonal variation of atmospheric ozone in India and some ozone-weather relationships. MAUSAM 14, 68–74. https://doi.org/10.54302/mausam.v14i1.5086

Ricchiazzi, P., Yang, S., Gautier, C., Sowle, D., 1998. SBDART: A Research and Teaching Software Tool for Plane-Parallel Radiative Transfer in the Earth's Atmosphere. Bull. Amer. Meteor. Soc. 79, 2101–2114. https://doi.org/10.1175/1520-0477(1998)079<2101:SARATS>2.0.CO;2

Ruiz-Arias, J.A., Alsamamra, H., Tovar-Pescador, J., Pozo-Vázquez, D., 2010.Proposal of a regressive model for the hourly diffuse solar radiation under all sky conditions. Energy Conversion and Management 51, 881–893. https://doi.org/10.1016/j.enconman.2009.11.024

Sadasivan, S., 1979.Trace elements in monsoon rains at Bombay and over the Arabian Sea. MAUSAM 30, 449–456. https://doi.org/10.54302/mausam.v30i4.3078

Sadasivan, S., 1980.Variation of trace element concentration in rainwater with rainfall rate and rainfall amount. MAUSAM 31, 222–224. https://doi.org/10.54302/mausam.v31i2.3838

Sarkar, J., Soni, V.K., Gadgil, A.S., Mukherjee, A.K., 2006. Analyzing rainwater chemistry at the continental GAW station Nagpur. MAUSAM 57, 653–662. https://doi.org/10.54302/mausam.v57i4.504

Sateesh, M., Soni, V.K., Raju, P.V.S., 2018a.Effect of Diwali Firecrackers on Air Quality and Aerosol Optical Properties over Mega City (Delhi) in India. Earth Syst Environ 2, 293–304. https://doi.org/10.1007/s41748-018-0054-x

Sateesh, M., Soni, V.K., Raju, P.V.S., Mor, V., 2018b. Cluster analysis of aerosol properties retrieved from a sky-radiometer over a coastal site: Thiruvananthapuram, India. Atmospheric Pollution Research 9, 207–219. https://doi.org/10.1016/j.apr.2017.09.002

Sateesh, M., Soni, V.K., Raju, P.V.S., Prasad, V.S., 2019.Analysis of Absorption Characteristics and Source Apportionment of Carbonaceous Aerosol in Arid Region of Western India. Earth Syst Environ 3, 551–562. https://doi.org/10.1007/s41748-019-00122-z

Satheesh, S., Ramanathan, V., Li-Jones, X., Lobert, J., Podgorny, I., Prospero, J., Holben, B., Loeb, N., 1999. A model for the natural and anthropogenic aerosols over the tropical Indian Ocean derived from Indian Ocean Experiment data. Journal of Geophysical Research: Atmospheres 104, 27421–27440.

Satheesh, S.K., Ramanathan, V., 2000. Large differences in tropical aerosol forcing at the top of the atmosphere and Earth's surface. Nature 405, 60–63. https://doi.org/10.1038/35011039

Sharma, A.K., Datta, S.M., Baluja, K.L., 2011. GLOBAL ANALYSIS OF LONG-TERM TRENDS IN TOTAL OZONE DERIVED FROM DOBSON OR GROUND BASED INSTRUMENT DATA. MAUSAM 62, 103–107. https://doi.org/10.54302/mausam.v62i1.215

Singh, Atinderpal, Tiwari, Shani, Sharma, D., Singh, D., Tiwari, Suresh, Srivastava, A.K., Rastogi, N., Singh, AK, 2016. Characterization and radiative impact of dust aerosols over northwestern part of India: a case study during a severe dust storm. Meteorology and Atmospheric Physics 128, 779–792.

Singh, D., Mukhopadhyay, B., Srivastava, H.N., 1997. Climatic impact on atmospheric turbidity at some Indian stations. MAUSAM 48, 33–40. https://doi.org/10.54302/mausam.v48i1.3827

Sinha, P., Bisht, A., Peshin, S., 2016.Long term trend in surface ozone over Indian stations. MAUSAM 67, 887–896. https://doi.org/10.54302/mausam.v67i4.1416

Sofiev, M., Vira, J., Kouznetsov, R., Prank, M., Soares, J., Genikhovich, E., 2015.Construction of the SILAM Eulerian atmospheric dispersion model based on the advection algorithm of Michael Galperin. Geosci. Model Dev. 8, 3497–3522. https://doi.org/10.5194/gmd-8-3497-2015

Soni, V.K., Bist, S., Bhatla, R., Bhan, S.C., Kumar, G., Sateesh, M., Singh, S., Pattanaik, D.R., 2018. Effect of unusual dust event on meteorological parameters & aerosol optical and radiative properties. MAUSAM 69, 227–242. https://doi.org/10.54302/mausam.v69i2.290

Soni, V.K., Kannan, P.S., 2003. Temporal variations and the effect of volcanic eruptions on atmospheric turbidity over India. MAUSAM 54, 881–890. https://doi.org/10.54302/mausam.v54i4.1588

Soni, V.K., Kannan, P.S., Ghanekar, S.G., Ravindran, U., Gaikwad, A.N., Lohogaonkar, S.M., Deshmukh, A.R.K., 2006. Long term variation in chemical composition of precipitation and wet deposition of major ions at Minicoy and Portblair : Islands in Arabian Sea and Bay of Bengal. MAUSAM 57, 489–498. https://doi.org/10.54302/mausam.v57i3.493

Soni, V.K., Pandithurai, G., Pai, D.S., 2012. Evaluation of long-term changes of solar radiation in India. Intl Journal of Climatology 32, 540–551. https://doi.org/10.1002/joc.2294

Soni, V.K., Pandithurai, G., Pai, D.S., 2016. Is there a transition of solar radiation from dimming to brightening over India? Atmospheric Research 169, 209–224. https://doi.org/10.1016/j.atmosres.2015.10.010

Soni, V.K., Sateesh, M., Das, A.K., Peshin, S.K., 2017.Progress in Meteorological Studies around Indian Stations in Antarctica.Proceedings of the Indian National Science Academy 90. https://doi.org/10.16943/ptinsa/2017/48954

Squizzato, S., Masiol, M., 2015. Application of meteorology-based methods to determine local and external contributions to particulate matter pollution: A case study in Venice (Italy). Atmospheric Environment 119, 69–81. https://doi.org/10.1016/j.atmosenv.2015.08.026

Sreekanth, V., Niranjan, K., Madhavan, B.L., 2007.Radiative forcing of black carbon over eastern India.Geophys. Res. Lett. 34, L17818. https://doi.org/10.1029/2007GL030377

Srivastava, A.K., Yadav, V., Pathak, V., Singh, S., Tiwari, S., Bisht, D.S., Goloub, P., 2014a. Variability in radiative properties of major aerosol types: A year-long study over Delhi—An urban station in Indo-Gangetic Basin. Science of The Total Environment 473–474, 659–666. https://doi.org/10.1016/j.scitotenv.2013.12.064

Srivastava, A.K., Yadav, V., Pathak, V., Singh, S., Tiwari, S., Bisht, D.S., Goloub, P., 2014b. Variability in radiative properties of major aerosol types: A year-long study over Delhi—An urban station in Indo-Gangetic Basin. Science of The Total Environment 473–474, 659–666. https://doi.org/10.1016/j.scitotenv.2013.12.064

Srivastava, H.N., Datar, S.V., Mukhopadhyay, B., 1992. Treands in atmospheric turbidity over India. MAUSAM 43, 183–190. https://doi.org/10.54302/mausam.v43i2.3382

Suresh Babu, S., Krishna Moorthy, K., Satheesh, S., 2007. Temporal heterogeneity in aerosol characteristics and the resulting radiative impacts at a tropical coastal station–Part 2: Direct short wave radiative forcing. Presented at the Annales Geophysicae, Copernicus Publications Göttingen, Germany, pp. 2309–2320.

Taneja, K., Attri, S.D., Ahmad, S., Ahmad, K., Soni, V.K., Mor, V., Dhankhar, R., 2017. Comparative assessment of aerosol optical properties over a mega city and an adjacent urban area in India. MAUSAM 68, 673–688. https://doi.org/10.54302/mausam.v68i4.767

Tiwari, S., Kaskaoutis, D., Soni, V.K., Dev Attri, S., Singh, A.K., 2018. Aerosol columnar characteristics and their heterogeneous nature over Varanasi, in the central Ganges valley. Environ Sci Pollut Res 25, 24726–24745. https://doi.org/10.1007/s11356-018-2502-4

Tiwari, V.S., 1999. Measurement of Ozone at Maitri, Antarctica. MAUSAM 50, 203–210. https://doi.org/10.54302/mausam.v50i2.1848

Tripathi, S.N., Pattnaik, A., Dey, S., 2007.Aerosol indirect effect over Indo-Gangetic plain. Atmospheric Environment 41, 7037–7047. https://doi.org/10.1016/j.atmosenv.2007.05.007

U.S. NAPAP, 1991.1990 Integrated assessment report. Office of the Director, National Acid Precipitation Assessment Program (US).

Verma, O.P., Kotwani, R., Ramanujan, S., 1970.CHEMICAL ANALYSIS OF RAIN WATER AT TEZPUR (ASSAM).MAUSAM 21. https://doi.org/10.54302/mausam.v21i4.5810

Verma, S., Prakash, D., Srivastava, A.K., Payra, S., 2017. Radiative forcing estimation of aerosols at an urban site near the thar desert using ground-based remote sensing measurements. Aerosol and Air Quality Research 17, 1294–1304.

Vinoj, V., Babu, S.S., Satheesh, S.K., Moorthy, K., Kaufman, Y.J., 2004. Radiative forcing by aerosols over the Bay of Bengal region derived from shipborne, island-based, and satellite (Moderate-Resolution Imaging Spectroradiometer) observations. J. Geophys. Res. 109, 2003JD004329. https://doi.org/10.1029/2003JD004329

Vyas, S.S., Bhattacharya, B.K., Nigam, R., 2016. Assured solar energy hot-spots over Indian landmass detected through remote sensing observations from Geostationary Meteorological Satellite. Current Science 836–842.

Wielicki, B.A., Barkstrom, B.R., Harrison, E.F., Lee III, R.B., Smith, G.L., Cooper, J.E., 1996. Clouds and the Earth's Radiant Energy System (CERES): An earth observing system experiment. Bulletin of the American Meteorological Society 77, 853–868.

WMO: Coupled Chemistry-Meteorology/Climate Modelling (CCMM): Status and Relevance for Numerical Weather Prediction, Atmospheric Pollution and Climate Research, Geneva, Switzerland, 23–25 February 2015, World Meteorological Organization, Geneva, ISBN 978-92-63-11172-2, 165 pp., 2016.

Yadav, B.R., 1965. Total Solar Radiation in relation to duration of sunshine. MAUSAM 16, 261–266. https://doi.org/10.54302/mausam.v16i2.5640

Zhang, Y., Bocquet, M., Mallet, V., Seigneur, C., Baklanov, A., 2012. Real-time air quality forecasting, part II: State of the science, current research needs, and future prospects. Atmospheric Environment 60, 656–676. https://doi.org/10.1016/j.atmosenv.2012.02.041.